5-2020

Computational Quantum Study of Intermediates Formed During the Partial Oxidation of Melatonin

Oladun Oladiran
East Tennessee State University

Computational Quantum Study of Intermediates Formed During the Partial Oxidation of Melatonin

_____

A thesis

presented to

the faculty of the Department of Chemistry

East Tennessee State University

In partial fulfillment

of the requirements for the degree

Master of Science in Chemistry

_____

by

Oladun Solomon Oladiran

May 2020

_____

Dr. Scott Kirkby, Chair

Dr. Marina Roginskaya

Dr. David Close

Keywords: Melatonin, Spin traps, Free Radicals, DFT, HF, Basis Set Extrapolation

ABSTRACT

Computational Quantum Study of Intermediates Formed During the Partial Oxidation of Melatonin

by

Oladun Solomon Oladiran

Melatonin is a neurohormone produced by the pineal gland in the brain. It functions as an antioxidant to scavenge free radicals. Free radicals are reactive species; they often oxidize the cells leading to oxidative stress which may lead to severe health complications. Reaction of melatonin with free radicals is known to be stepwise, as such the stability of the intermediates can be examined. Thus, the possibility of using melatonin as an *in vivo* spin trap can be determined. Spin traps allow characterization of unstable radical species using electron spin resonance spectroscopy. In this research, *ab initio* quantum chemistry techniques were used to calculate the energies of selected intermediates formed during the partial oxidation of melatonin by hydroxyl radical. Specifically, optimized geometries for melatonin, and selected intermediates with ·OH were obtained at the DFT/B3LYP/cc-pVXZ and HF/cc-pVXZ (X = D, T, Q) levels of theory. Extrapolations to the complete basis set limit were also performed.

DEDICATION

This work is dedicated to all my loved ones…

ACKNOWLEDGEMENTS

First, I would like to express my deepest gratitude to my advisor, Dr. Scott Kirkby, for his patience, motivation, immense knowledge, and unwavering support during and towards the completion of this thesis. His guidance and supervision were valuable for the success of the research and in the writing of this thesis.

Besides my advisor, I would also like to thank my committee members: Dr. Marina Roginskaya and Dr. David Close for their encouragement, as well as, insightful comments. I want to especially thank Dr. Roginskaya both as my committee member and as a former graduate coordinator. Her advice is always useful, and I couldn't have succeeded without it.

I wouldn't forget my friends and classmates who have made this graduate school journey pleasant. I would like to thank Adeyemi Adeyelu for being very supportive even when it was not convenient. I appreciate all of your help and mentoring during my graduate program and before I came to the United States.

I also want to my express my sincere gratitude to the ETSU Department of Chemistry for the financial assistance provided in the form of a graduate assistantship.

Last but not the least, is my family; my parents, my brother, my cousins and my sisters. Thank you for the emotional support. I especially appreciate my mother for love and support both spiritually and physically during my graduate studies.

TABLE OF CONTENTS

LIST OF TABLES

Page

LIST OF FIGURES

Page

LIST OF ABBREVIATIONS

MLT:	Melatonin
AMK:	N^1-acetyl-5-methyoxykynuamine
AFMK:	N^1-acetyl-N-formyl-5-methoxykynuramine
DFT:	Density Functional Theory
CBS:	Complete Basis Sets
B3LYP:	Becke's Three Parameter Lee Yang Parr Functional
DMPO:	5, 5-dimethy-1-pyrroline N-oxide
EPR:	Electron Paramagnetic Resonance(spectroscopy)
ESR:	Electron Spin Resonance (spectroscopy)
GGA:	Generalized Gradient Approximation
GTO:	Gaussian Type Orbital
GTF:	Gaussian Type Function
H_2O_2:	Hydrogen peroxide
·OH:	Hydroxyl radical
NO·:	Nitric oxide radical
HO-MLT:	Hydroxymelatonin
KS:	Kohn-Sham
LC:	Linear Combination
LDA	Local Density Approximation
LSDA:	Local Spin Density Approximation
HOMO:	Highest Occupied Molecular Orbital
LUMO:	Lowest Unoccupied Molecular orbital
DZ:	Double Zeta
TZ:	Triple Zeta
QZ:	Quadruple Zeta
SCF:	Self Consistence Field Theory

RHF:	Restricted Hartree-Fock
HF:	Unrestricted Hartree-Fock
STO:	Slater Type Orbital
PBN:	N-tert-butyl-α-phenylnitrone

CHAPTER 1. INTRODUCTION

Free Radicals

Free radicals are atoms, molecules, or ions that have one or more unpaired electrons. This unpaired electron makes them very reactive towards non-radical reactive species such that they can either donate or accept electrons from other molecules.[1,2] These characteristics make them behave as oxidants as well as reductants, respectively.[3]

Free radicals are generated via two mechanisms: homolytic cleavage and electron transfer. However, the latter is the only mechanism available for the formation of free radicals in biological cells. Free radicals are categorized into reactive oxygen species (ROS) such as superoxide anion ($O_2^{\cdot -}$), hydroxyl radicals (·OH), peroxyl radicals (ROO·), hydrogen peroxide H_2O_2, peroxynitrite $ONOO^-$, and alkoxy radical $RO^{\cdot}$ and reactive nitrogen species (RNS) radical such as nitric oxide radical (NO·**)**.

The existence of radical species in biological systems, especially at high concentration is known to be detrimental to the biological system because they attack the DNA, lipids, proteins, nucleic acid, etc. These attacks usually lead to oxidative stress which is a major contributor to several health problems including cancer,[4] neurodegenerative diseases[5] such as Alzheimer's,[6-7] and Parkinson's,[7] cardiovascular diseases,[8] aging,[9] and chronic obstructive pulmonary diseases.[10] However, in moderate concentrations, free radicals can be useful for processes such as cellular signaling systems, maturation of cellular structures and mitogenic responses, and in the apoptosis of defective cells.[11-12]

The small sizes of these radicals make them particularly harmful to biological systems since they can penetrate cell membranes easily and cause damage to the cells. Free radicals are mostly generated internally, due to metabolic processes in the human body such as those from the mitochondria[13], xanthine oxidase[14] and in the endoplasmic recticulum.[15] However, some external factors such as air pollutants, exposure to industrial chemicals, exposure to X-rays and ozone can contribute to the generation of free radicals in the body.[16]

This process occurs as a result of the enzymatic reduction of the oxygen thereby generating a reactive radical species.[17] An example of such, is the enzyme NAD(P)H oxidases.[18] A non-enzymatic compound such as the semi-ubiquinone compound can also aid the production of free radicals. Reactive nitrogen species can also exist but mostly in the higher organism and produced by the oxidation of one of the terminal guanidino nitrogen atoms of L-arginine.[19]

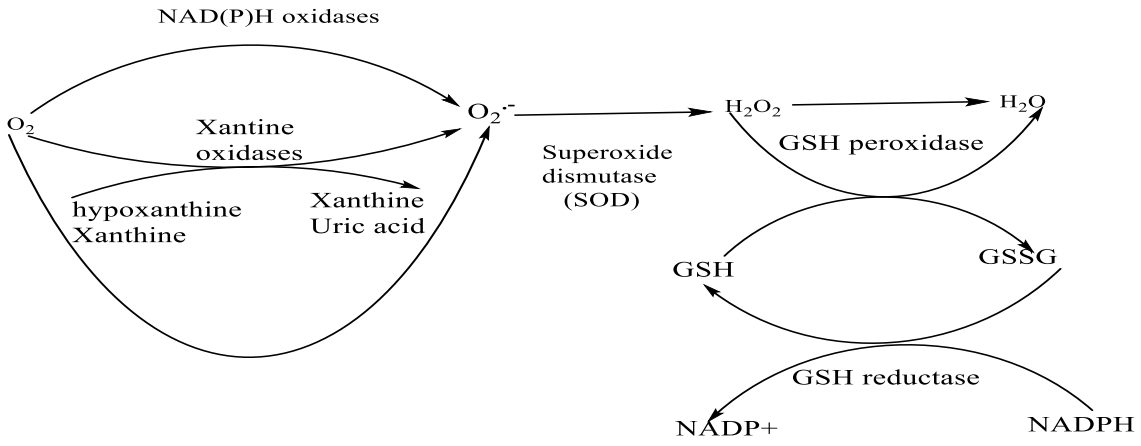

Figure 1. Pathways of reactive oxygen species (ROS) production and clearance. GSH, glutathione; GSSG, glutathione disulfide.

Reactive Oxygen Species

Reactive oxygen species (ROS) are a group of short-lived free radicals which are derived from oxygen. They are highly reactive molecules because of the presence of unpaired electrons in their valence shell. The reactive oxygen species are by far the most abundant and harmful free radicals. This is because they are obtained from the normal metabolism that occurs in the body as a result of oxygen-induced oxidization, generating free radicals. Examples of such radicals include superoxide anion, $O_2^{\cdot -}$, and hydroxyl radical, $^{\cdot}OH$. Hydrogen peroxide, H_2O_2 is also regarded to be a ROS, even though it does not have unpaired electrons, because it has the potential to generate hydroxyl radicals. To minimize the effect of the oxidants, the body exhibits defense mechanisms such as the production of antioxidants which can remove/scavenge the reactive oxygen species from the intracellular environment.[20]

However, when the defense mechanisms are insufficient for the number of oxidants available in the body, the result is oxidative stress. Oxidative stress is thought to lead to various undesired processes in the body and thus result in various complications such as aging, chronic renal failure, etc. In the study of radicals, superoxide anion ($O_2^{\cdot -}$) and hydroxyl radical ($^{\cdot}OH$) have received more attention owing to several controversies on the origin of the radicals. $O_2^{\cdot -}$ is thought to be the initial stage in the production of the ROS and ultimately the generation of the highly reactive and short lived free radical: the hydroxyl radial, $^{\cdot}OH$. It was proposed that the superoxide anion interacted with peroxide to generate hydroxyl radical, which is a very strong oxidizer.[20]

The Haber-Weiss reaction also describes the formation of hydroxyl radicals.[21] This reaction proceeds in the presence of Fe^{2+} salts and was first proposed by Henty J. Fenton in 1894 when he observed the oxidation of tartaric acid by H_2O_2 in the presence of iron (II) salts.[22]

An elaborated version of the Haber-Weiss reaction which includes the Fenton reaction was later proposed by Barb *et al.*[23] The mechanism of the Fenton reaction is given below.

$$Fe^{2+} + H_2O_2 \longrightarrow Fe^{3+} + OH^- + \dot{H}O \quad (1.1)$$

$$Fe^{3+} + H_2O_2 \longrightarrow Fe^{2+} + H^+ + H\dot{O}_2 \quad (1.2)$$

$$H\dot{O} + H_2O_2 \longrightarrow H\dot{O}_2 + H\bar{O}_2 \quad (1.3)$$

$$H\dot{O} + Fe^{2+} \longrightarrow Fe^{3+} + H_2O_2 \quad (1.4)$$

$$H\dot{O} + Fe^{2+} \longrightarrow Fe^{3+} + O_2H^+ \quad (1.5)$$

$$Fe^{2+} + H\dot{O}_2 + H^+ \longrightarrow Fe^{3+} + H_2O_2 \quad (1.6)$$

$$H\dot{O}_2 + H\dot{O}_2 \longrightarrow H_2O_2 + O_2 \quad (1.7)$$

Scientists have proposed a new mechanism (old Fenton reaction revisited)[24] which is a general description of the Fenton reaction because the same mechanism was observed for most transition metals such as manganese, copper, and cobalt. The use of iron was because of its presence in all biological media[25]. In the mechanism below, M represents transition metals.

$$M^{n+} + H_2O_2 \longrightarrow M^{(n+1)+} + \dot{O}H + OH^- \quad (1.8)$$

Hydroxyl Radical Reactions

Hydroxyl free radicals are short-lived, both in biological systems (half-life of about 10^{-9} s), and in the atmosphere (half-life range of about 0.01-1 s).[26] This is because they are the most reactive chemical intermediates known, as hydroxyl radical oxidizes many organic molecules

and as such it finds several applications in chemistry and biology, organic synthesis, photocatalysis, wastewater treatment, and many other chemical processes.[27-28] Like many radicals, its reaction with molecules is usually by addition reactions with the unsaturated substrate, however abstraction of hydrogen is also favorable.[29]

The reactions are particularly of interest in biological systems since the hydroxyl radical can attack DNA by addition to pyrimidine nucleobases causing extensive damage to the DNA/RNA.[30] Sesil *et al.*[31]studied the reaction of hydroxyl radical with diclofenac (DCF).

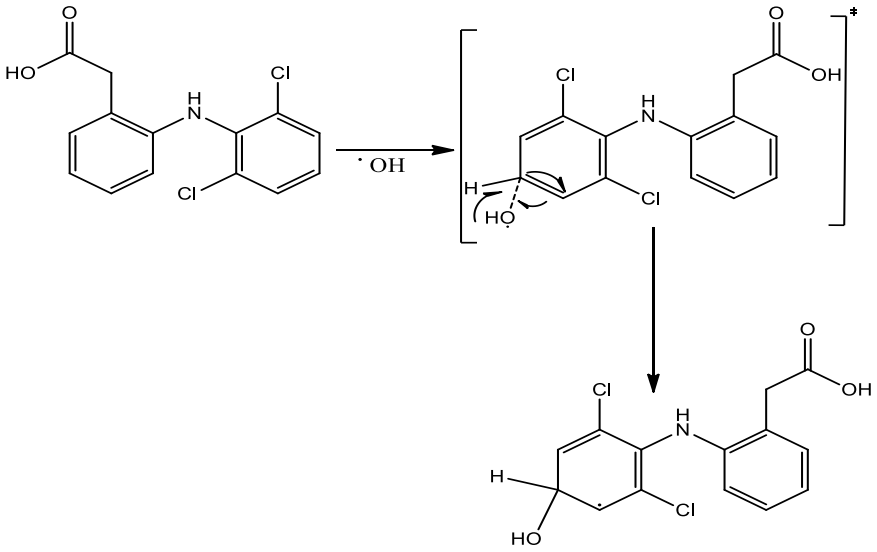

Figure 2. Addition reaction of hydroxyl radicals with DCF to generate radical intermediate

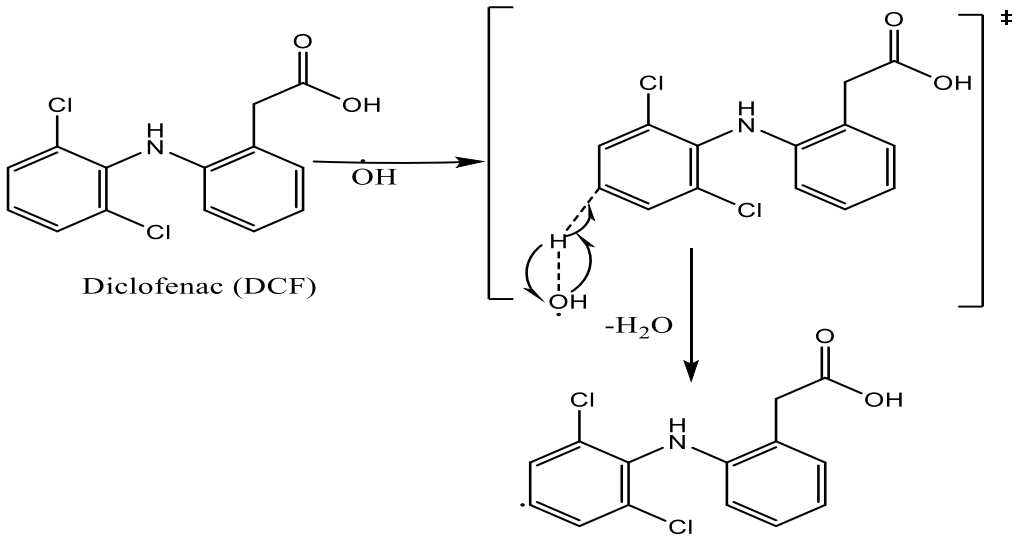

Figure 3. Hydrogen- abstraction by hydroxyl radical to generate radical intermediate.

Hydroxyl radical also undergoes electron transfer reactions with aromatic compounds in aqueous solution

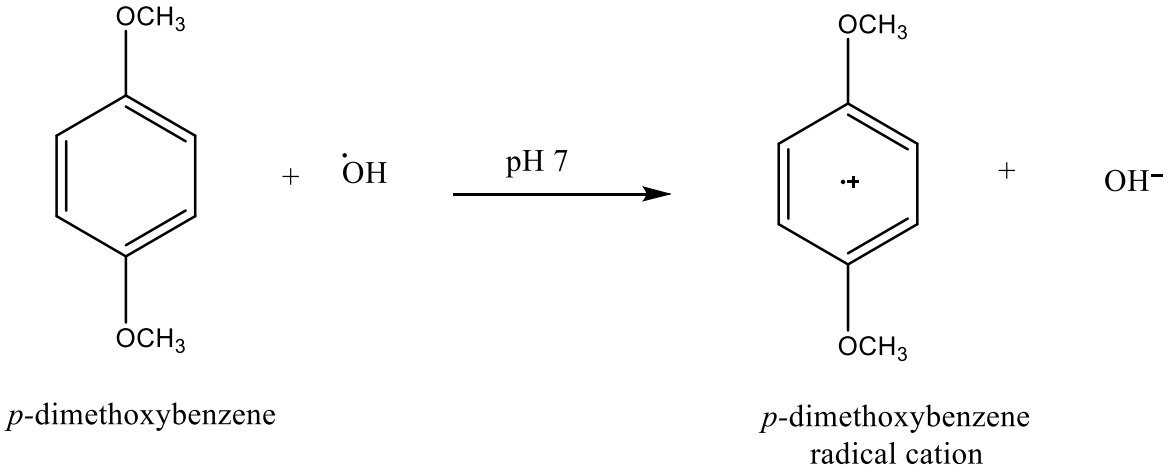

Figure 4. Electron transfer reaction by hydroxyl radical to generate reactive intermediate

Spin Traps

Spin traps react with transient free radicals to obtain a more stable radical adduct. Since most radical are short-lived, spin trapping the radical allows easy characterization of by indirect method such as using Electron paramagnetic spectroscopy.[31-32] In biological systems, there are radical scavengers or antioxidants. These include superoxide dismutase (SOD), catalase (CAT), gluthathione reductase (GR) etc. and they are useful for the removal of excess free radical from the living cells thereby ensuring good and healthy cells.[34] These regular antioxidants can be used as spin traps, however, not all radical scavengers can be used as spin traps and some have been found to react insdiscriminately with both oxygen and ROS producing excess water and subsequently leading to hypoxia (lack of oxygen) in deep tissue.[35]

Spin traps, on the other hand, selectively scavenge only free radicals such that the radical spin adduct can be analyzed. Since radicals such as the hydroxyl radical have a short lifetime, using a spin trap molecule stabilizes and lengthens the radical lifetime so that the resulting radical intermediate can be detected by Electron Paramagnetic Resonance (EPR) spectroscopy.[36] The stable radical formed cannot take part in further oxidative processes and as such, they are useful as preservatives in food, cosmetics, pharmaceutical, and other industries. Generally, the reaction can be written in its simplest form to produce a radical spin adduct

$$\underset{\text{(spin trap)}}{R^{\bullet} + ST} \longrightarrow \underset{\text{(spin adduct)}}{R{-}SA^{\bullet}} \qquad (1.9)$$

The use of spin traps for *in vitro* 'trapping' of free radicals being has been documented[37] and several spin trapping agents have been identified, these include nitrones e.g. hydroquinone,[38] edaravone,[39] phenyl tert-butylnitrone (PBN)[40], 5,5-dimethyl-1-pyrroline *N*-oxide (DMPO), and

many nitroso compounds such as 2,3,5,6-tetramethyl nitrobenzene (nitrosodurene, ND), 2,3,6-tri-tert-butyl nitrosobenzene (BNB), and sodium 3,5-dibromo-4-nitrosobenzene sulphonate (SBNS).[41] However, the most common spin traps are PBN and DMPO, because they are thermally and photochemically stable and very soluble in polar and non-polar solvents. [42-44] Besides, the *in vitro* applicability of these spin traps, their use in *in vivo* conditions has also been verified.[45-46]

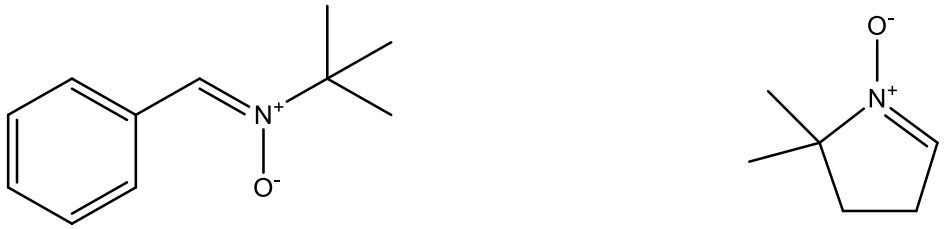

A. PBN derivatives B. DMPO derivatives

Figure 5. Structures of the two most common spin traps families, A. *N*-tert-butyl-α-phenylnitrone (PBN), B. 5,5-dimethyl-1-pyrroline *N*-oxide (DMPO)

Melatonin

Melatonin (N-acetyl-5-methoxytryptamine), a derivative of the amino acid tryptophan,[47] is a hormone which is produced in the brain by the pineal gland,[48] especially during dark times.[49] It was first isolated in 1958 by Lerner *et al.*[50] from the bovine pineal glands and the structure was determined in 1959.[51-52]

The production of melatonin in mammals involves the catalytic hydroxylation of the amino acid tryptophan by the enzyme trytophan hydroxylase to yield 5-hydroxytrptophan. This initial product can be further decarboxylated to form serotin by aromatic L-amino-acid

decarboxylase.[53] Arylalkylamine N-acetyltransferase and hydroxyindole-O-methylfransferase catalysed the acetylation and ethylation of serotin to produce melatonin.[54-55]

The production of melatonin is not, however, limited to the pineal gland; some tissues, cells and body fluids contain exceptionally high levels of melatonin. Examples include the retina[52] as well as skin,[56] platelets,[57] lympocytes,[58] gastrointestinal tract,[59] and bone marrow.[60-61] In fact, some of these have melatonin concentrations multiple times more than is found in the blood, for example, bile[62] and cerebrospinal fluid.[63]

Due to the multiple sites of formation, melatonin receptors are in diverse locations leading to extensive control of several physiological process.[64-65] including sleep and the circadian rhythm,[66 -67] reproduction,[68] and immune system responsiveness.[69] Other than the presence of melatonin in humans, it is also known to exist in some lower organisms such as fungi,[70] algae,[71] protista[72] as well as some in cells of plants and other mammals.

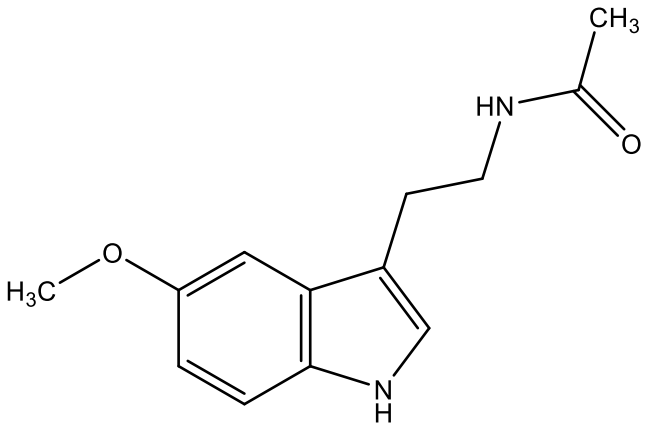

Figure 6: Structure of melatonin

Melatonin is also known to be an antioxidant/free radical scavenger in addition to its numerous functions stated earlier.

The role of melatoninn as an antioxidant was first proposed in 1991 by Ianas *et al.*[73] and was later confirmed as a direct radical scavenger in 1993 by Hardeland *et al.*[74]

The efficiency of melatonin as an antioxidant is obvoius for many reasons; it has very low to no toxicity in the body or in its long-term administration.[75] Also, due to its high solubility in lipids and partial solubility in water, melatonin can pass through many physiologic barriers.[76-77] Its antioxidant ability does not decrease after its oxidation since its metabolites also exhibit antioxidant capacity.[78] *In vivo* antioxidant ability of melatonin can occur directly by scavenging radicals and/or inhibiting their formation or indirectly by upregulating endogenous antioxidant defenses.[79] Evidence of *in vitro* antioxidant ability of melatonin through a Fenton-like reaction in the presence Cu(II)/H_2O_2 was reported by Kladna *et al.*[80] The main oxidation product N^1-acetyl-N ^{2}-formyl-5-methoxykynurenine (AFMK), N^1-acetyl-5-methoxykynurenine (AMK), and hydroxyl melatonin (HO-MLT)[81]

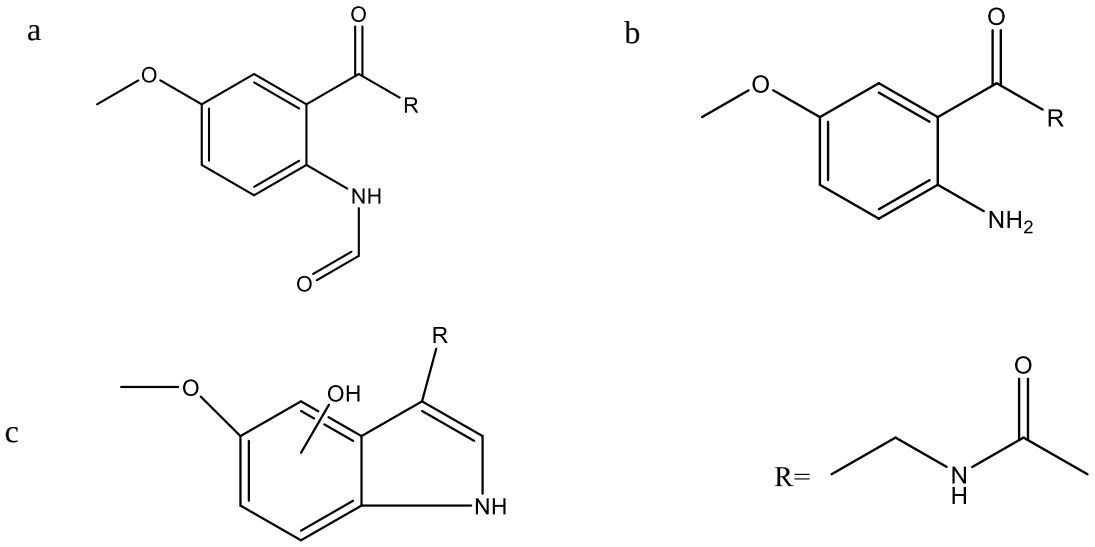

Figure 7: Structures of melatonin's oxidation products; **a**: N^1-acetyl-N 2-formyl-5 methoxykynurenine (AFMK), **b**: N^1-acetyl-5-methoxykynurenine (AMK) **c**: Hydroxymelatonin

Mechanism of Reaction Between Melatonin and Free Radicals

There is limited information documented for mechanisms describing the antioxidant activity of melatonin. However, based on information from other antioxidants, a plethora of possibilities have been proposed: radical adduct formation (RAF), hydrogen atom transfer (HAT), single electron transfer (SET), proton coupled electron transfer (PCET), and sequential electron proton transfer (SEPT).[82]

Radical adduct formation (RAF):

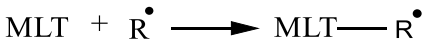

(1.10)

Hydrogen atom transfer (HAT):

(1.11)

Single electron transfer (SET):

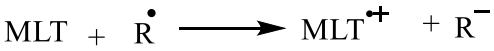

(1.12)

Proton coupled electron transfer (PCET):

(1.13)

Sequential electron proton transfer (SEPT):

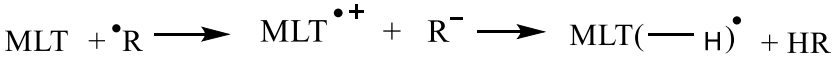

(1.14)

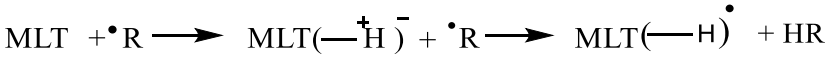

(1.15)

Oxidation of Melatonin

Melatonin reactivity towards free radicals leads to oxidation products, some of which are equally or even more effective as radical scavengers than the parent melatonin.[83] As stated earlier, the main oxidation products of MLT are AFMK and AMK. The reaction path is known to occur via the conversion of serotonin by N-acetyl transferase (NAT) to N-acetyl serotonin. The N-acetyl serotonin formed is further converted to melatonin by hydroxyindole O-methyl transferase (HIOMT) and subsequently AFMK, AMK, 3-OH-MLT(cyclic), and 6-OH-MLT.[84]

The reverse reaction is also possible making NAT a metabolite of melatonin possessing antioxidative capability independent of that from melatonin.[85-86] According to computational studies by Zavodnik *et al*.[87] using AMI and RHF methods, AFMK is the most stable oxidation product. The oxidation of melatonin for the production AFMK was studied by Reiter *et al.*[88] He proposed two pathways; first through the direct addition of $^1O_2$ to form dioxetane intermediates and the other by via diol and epoxide intermediates. 6-OH-MLT- a metabolite of oxidation of melatonin is known for its high radical scavenging compared to melatonin.[88-89] In fact, it is reported to scavenge both singlet oxygen and superoxide anion which are particularly resistant to melatonin, thereby reducing the quinolic-acid induced oxidative neurotoxicity.[90]

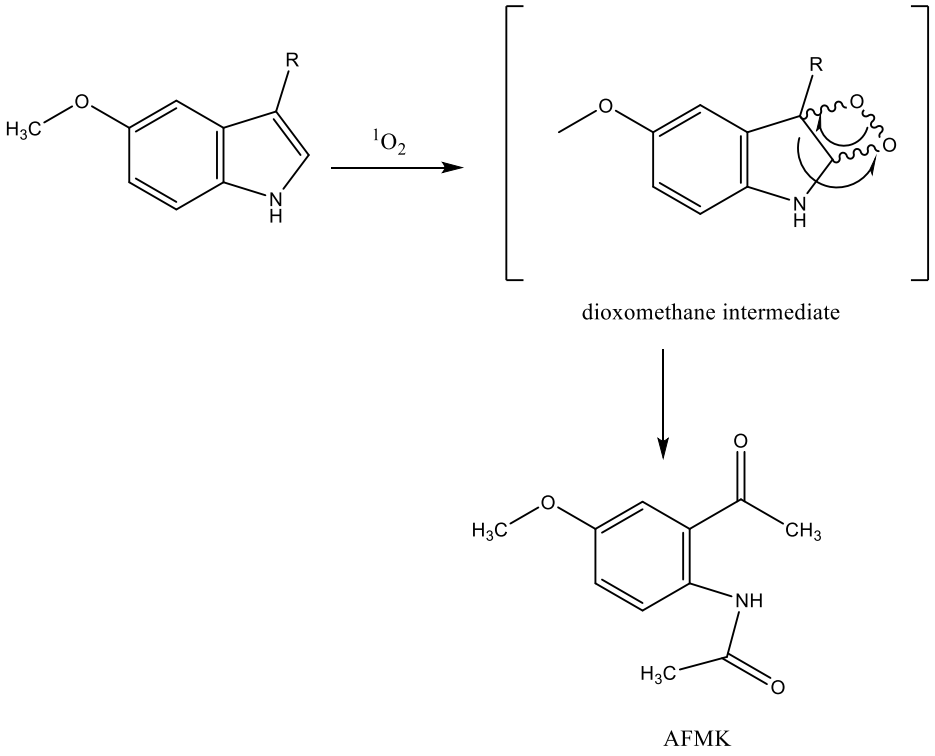

Figure 8: Proposed mechanism for MLT via an intermediate that decomposes to yield AFMK

The mechanism of its reaction with free radicals has been found to proceed via the HAT mechanism. The physico-chemical study of 6-OHMLT as protection against oxidative stress by Àlvarez-Diduk *et al.*[84] showed that the HAT path is the most thermodynamically stable since reaction involving phenolic OH are predicted to be exergonic

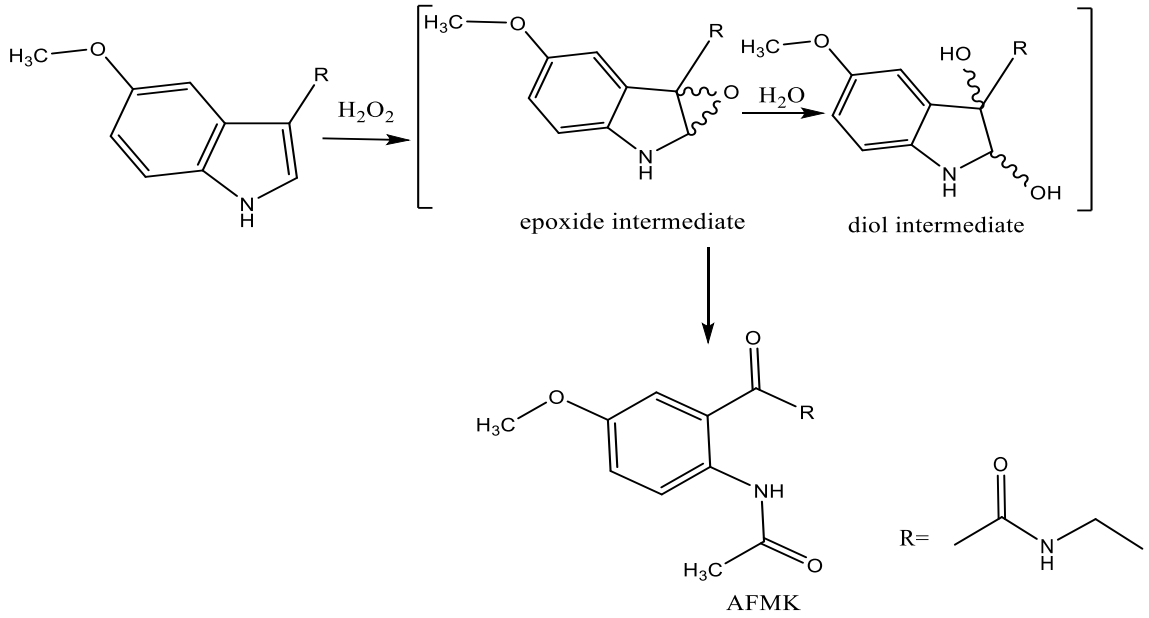

Figure 9: Oxidation of melatonin to AFMK via the epoxide and diol intermediate

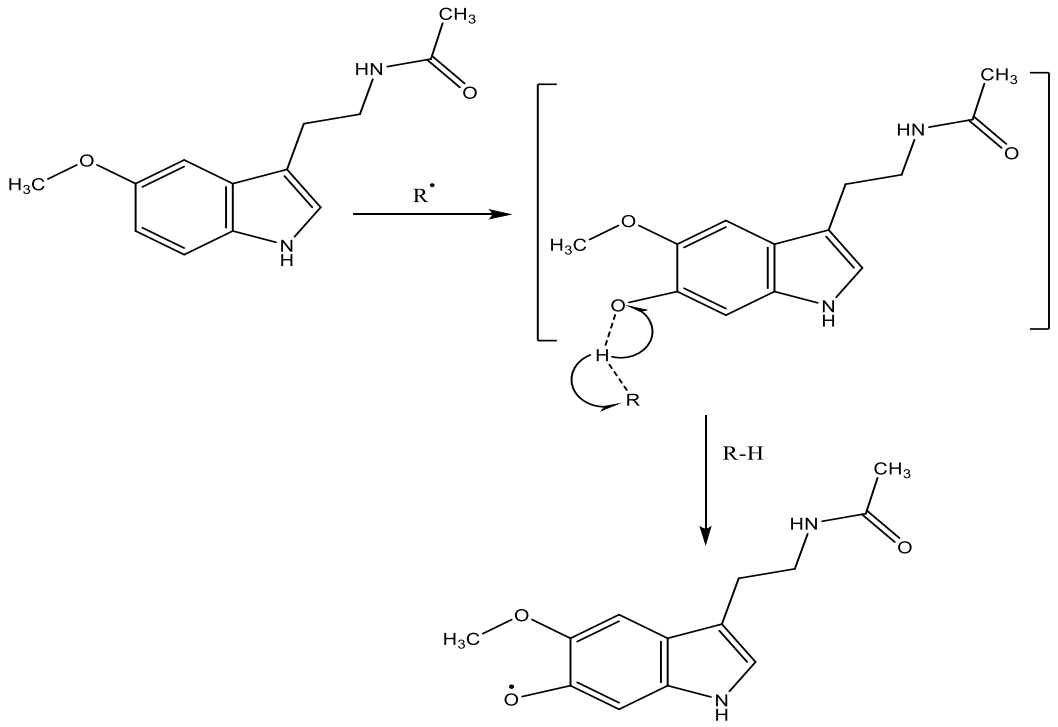

Figure 10: HAT mechanism pathway of the reaction of 6-OH melatonin with a free radical

Partial Oxidation of Melatonin by Hydroxyl Radical

Hydroxyl radical is known to as one of the most reactive species in the biological system and capable of oxidizing the cells. However, melatonin has been identified to successfully scavenge this reactive species. The antioxidant ability against hydroxyl radicals is well documented in many researches such as the work of Hardeland *et al.*[73], Turjanski *et al.*[79], Allegra *et al.*[91] and many others. Galano *et al.*[92] identified cyclic 3-OH MLT as the major product of the oxidation of melatonin by hydroxyl radical. However, other products have also been identified. During the oxidation of melatonin by hydroxyl radical, several paths have been proposed and may result in different oxidation products. In many cases, the hydroxyl radical may attack positions C2, C4, C6 or C7. Hardeland *et al.*[73] proposed an indolyl cation radical pathway but

the computational study by Turganski *et al.*[79] found the path to be thermodynamically unfavorable.

They however, proposed a radical addition pathway in which neutral indolyl radical is formed and found this path to be thermodynamically feasible. Due to radical stabilization,[93] positions C2, C4, and C6 could be favored. The proposed mechanism for the radical addition path is indicated in Figures 11,12 and 13. While our mechanism involves a radical addition, the use of hydroxyl radical for hydrogen abstraction to produce water is a "stand in" for any possible abstraction routes.

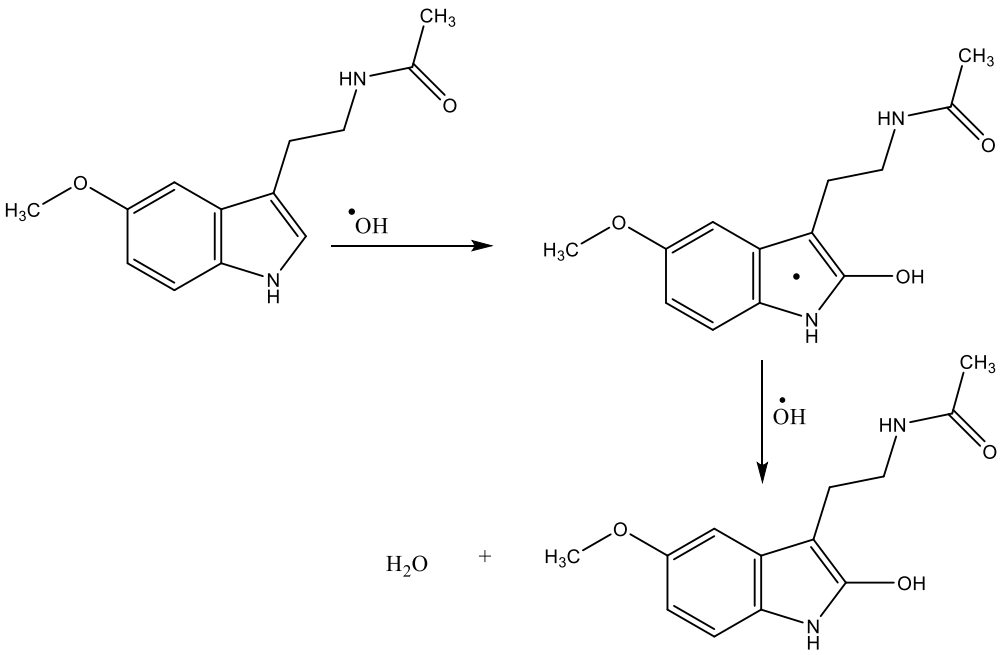

Figure 11: Proposed reaction path to the production 2-OH melatonin

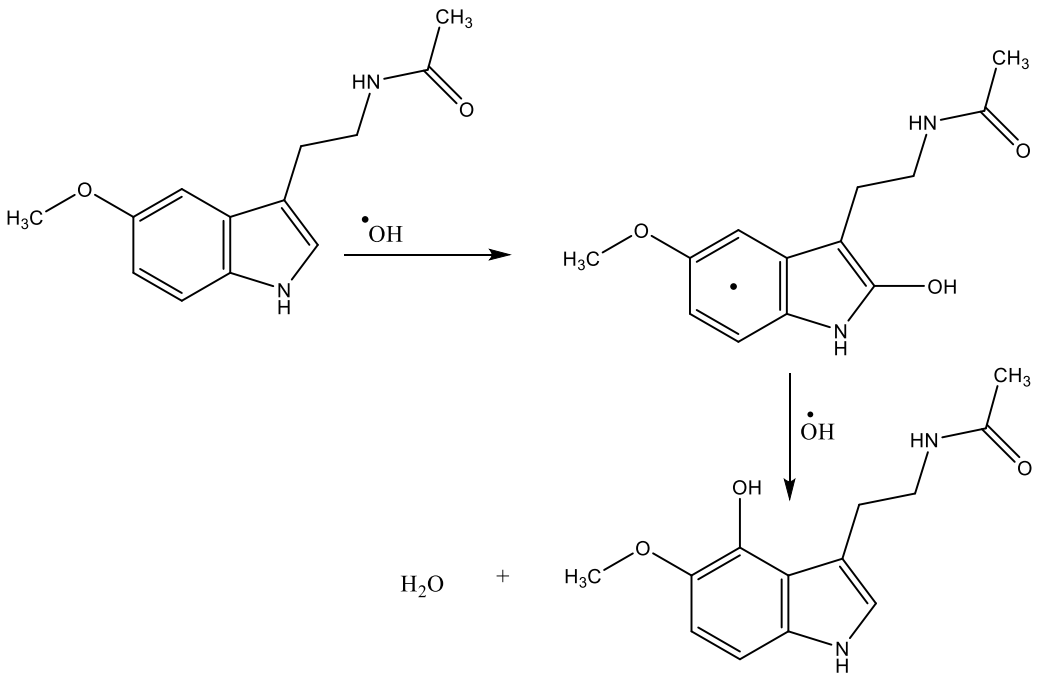

Figure 12: Proposed reaction path to the production of 4-OH melatonin

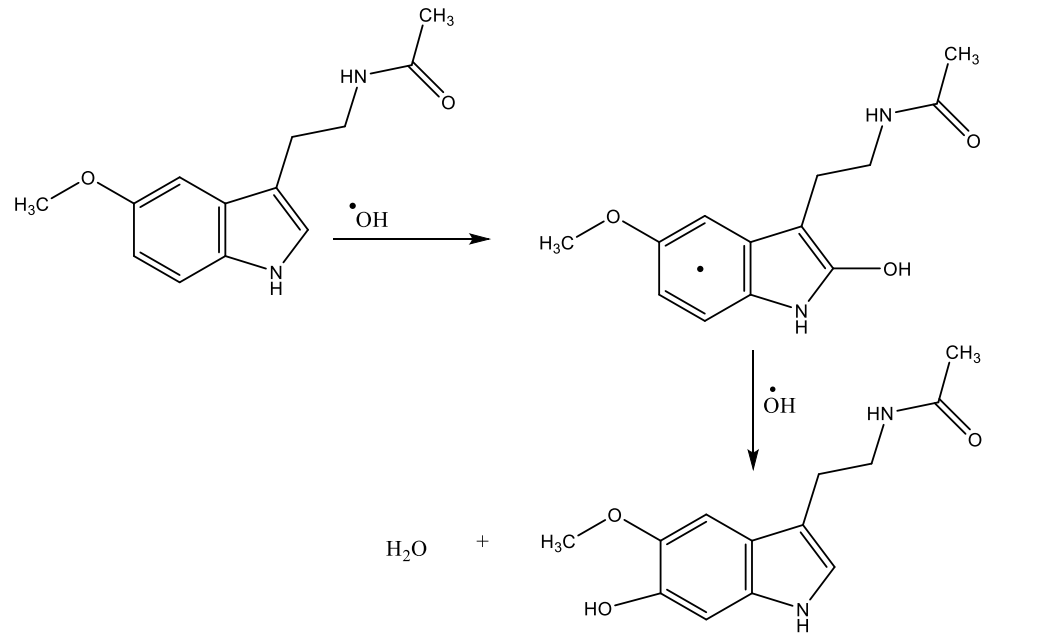

Figure 13: Proposed reaction path to the production of 6-OH melatonin

Review of Computational Studies of Melatonin Oxidation

A computational study conducted by Miglivacca *et al.*[94] supported the antioxidant efficacy of melatonin as revealed by semi-empirical and *ab initio* quantum-mechanical calculations. In the work, the electron transfer capabilities and stability of the radical formed by hydrogen abstraction were determined by calculating the relative ionization potential and relative O-H bond dissociation enthalpy, respectively. Conformers were identified by a quenched MD exploration and further optimized to the semi-empirical level using Hartree-Fock approximation in restricted and unrestricted modes. The results presented from the calculations showed that other than electrostatic interactions, hyperconjugation also accounts for the stabilization of the radical cation of some of the conformers of melatonin and in turn improves antioxidant efficacy.

Galano investigated the electron donor ability of synthetic MLT derivatives compared to parent MLT. [95] Density Functional Theory (DFT) was used in the calculation to test for 37 MLT derivatives. Fourteen DFT approximations were made to determine the best approximation method. The LC-ωPBE functional was found to be the most appropriate, and 6-311+G(d) was also used in conjunction with it. The electron donor ability of the compounds was quantified using an equivalent of the ionization energy in aqueous medium. The calculated ionization energies in aqueous solution showed very high ionization energy for MLT derivatives compared to the parent MLT. This can be related to an electron donating effect made effective by donating groups attached to the benzene ring. Particularly, it was found that OH groups and halogens attached to the benzene ring provide better electronic effect and hence better antioxidant activity.

Research Aim

Reaction of melatonin with hydroxyl radical is very important in biological systems. Melatonin can scavenger the hydroxyl radical, thus prevent further oxidation of the cells. However, the reaction mechanism is still not clear and several routes to oxidation of melatonin have been proposed. Studies have shown that there may be three oxidation products during the partial oxidation of melatonin: 2-OH-MLT, 4-OH-MLT and 6-OH-MLT.

The aim of the research is examining the intermediate formed during the partial oxidation of melatonin, this will consequently give insight to how melatonin could possibly be used as spin traps. To do this, computational methods, which are relatively inexpensive as compared to experimental methods, will be used to examine reactivity at the molecular level.

The work focuses specifically on the comparison of the energy of intermediates in gas phase produced during the partial oxidation of melatonin with hydroxyl radical at C2, C4, and C6 positions. Geometry optimizations were performed at the DFT/B3LYP/6-31G, DFT/B3LYP/6-31G(d), HF/cc-pVDZ, HF/cc-pVTZ, and single point molecular energy calculations was performed at the DFT/B3LYP/cc-pVQZ and HF/cc-VQZ levels of theory. The optimized geometry calculations were extrapolated to the complete basis set at the HF/cc-VXZ= (X=D, T, Q) and DFT/B3LYP/cc-pVXZ (X=D, T, Q).

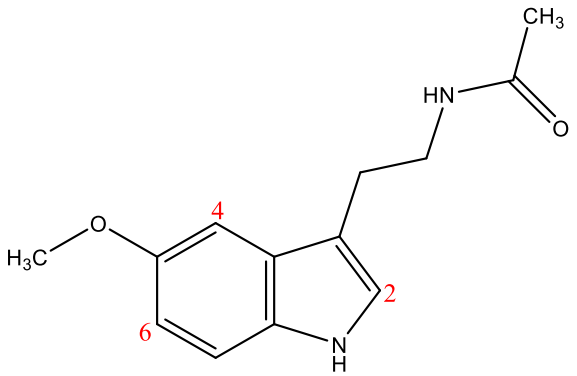

Figure 14: Structure of melatonin showing possible reaction sites with hydroxyl radical

CHAPTER 2. QUANTUM MECHANICS

Schrödinger Equation

Early scientists such as Isaac Newton and James Maxwell described the behavior of particles at the macroscopic level. This classical view of particles allows us to predict accurately the future state of the particles from a simple experiment. For example, Newtonian mechanics predicts the momentum of a particle given the mass of the particle. In fact, Newton's second law, states that the future state and future motions of a system at any time can be precisely determined. This idea makes classical mechanics deterministic in nature. The question is how we can explain the behavior of a wave or particles that behave in a wavelike manner especially particles at the microscopic level. In fact, classical mechanics failed to explain blackbody radiation and the photoelectric effect.

The emergence of quantum mechanics provides a better explanation of phenomena that could not be explained by classical mechanics. Quantum mechanics uses the idea of probability to explain the behavior of microscopic particles. In 1927, Werner Heisenberg further elucidated the behavior of particles at this level when he proposed the Heisenberg uncertainty principle. For, example, we cannot simultaneously measure with certainty, the position and the velocity/momentum of microscopic particles. Hence quantum mechanics, as opposed to classical mechanics, is not deterministic but probabilistic.

In Schrödinger's formulation of quantum mechanics, a wave function is used to describe the state of the system.[96] The wave of the system is described by the wave function (Ψ).

The time-dependent Schrödinger equation established the evolution with time of the wave function.[97-98]

$$\frac{-\hbar^2}{2m}\frac{\partial^2\Psi(x,t)}{\partial x^2} + V(x,t)\Psi(x,t) = -\frac{\hbar}{i}\frac{\partial\Psi(x,t)}{\partial t} \tag{2-1}$$

where ħ is the reduced Plank's constant equal to $\frac{h}{2\pi}$, i is the imaginary operator $\left(i = \sqrt{-1}\right)$, m is the mass of the particle, ∇^2 is the second order differential operator also known as the Laplacian operator and is given as:

$$\nabla^2 = \frac{\partial^2}{\partial \mathrm{x}^2} + \frac{\partial^2}{\partial \mathrm{y}^2} + \frac{\partial^2}{\partial \mathrm{z}^2} \tag{2-2}$$

As indicated earlier, the precise future state of a particle cannot be determined given the wavefunction. However, the probability density, $|\Psi|^2$, of the particle can be determined. This explains the non-deterministic property of the particle and thus gives the probability of finding a particle in a region. The absolute square of the quantity is the product of the quantity itself and its complex conjugate.

$$|\Psi|^2 = \Psi^*\Psi \tag{2-3}$$

Ψ^* is the complex conjugate formed by replacing i with $-i$. In-fact, Max Born proposed the probability of finding a particle at a given time within a region x and $x + dx$ in one dimension is given as:[99]

$$\Psi^*(x,t\,)\Psi(x,t)dx = |\Psi(x,t)|^2 dx \tag{2-4}$$

Assuming the particle is in some finite region, the sum of probabilities of finding the particles must be equal to 1, since the particle must be present somewhere in the in the region.

$$\int_{-\infty}^{\infty} |\Psi|^2 dx = 1 \tag{2-5}$$

A normalization of the wave function $\Psi = N\phi$ can be achieved by multiplication by the normalization constant N

$$\int_{-\infty}^{\infty} |\phi|^2 dx = |N|^{-2} \tag{2-6}$$

In quantum mechanics, the time-independent Schrödinger equation has proven to be more useful than the formidable time-dependent Schrödinger equation. This is especially true when the system does not experience time dependent external forces but rather when the potential energy function is a function of position $V(x)$ only. Hence the wave function can be separated into time, $f(t)$, and spatial, $\psi(x)$, functions.

$$\Psi(x,t) = \psi(x)f(t) \tag{2-7}$$

Substituting Equation 2-7 into 2-1 and differentiating with respect to time, yields

$$\frac{-\hbar}{i}\frac{1}{f(t)}\frac{df(t)}{dt}\psi(x) = \frac{\hbar^2}{2m}f(t)\frac{d^2\psi(x,t)}{dx^2} + V(x)\psi(x)f(t) \tag{2-8}$$

Dividing both sides by $\Psi(x,t) = \psi(x)f(t)$ gives

$$\frac{-\hbar}{i}\frac{1}{f(t)}\frac{df(t)}{dt} = \frac{1}{\psi(x)}\frac{d^2\psi(x,t)}{dx^2} + V(x) \tag{2-9}$$

In Equation 2-9, the left side is independent of x , therefore this function must also be independent of x . Also, the right side of the equation does not depend on t, therefore this function must also be independent of t. This must be a constant since the function is independent of both variables x and t. This constant can be called E. Multiplying both sides by ψ(x) gives the time-independent Schrödinger equation for a particle of mass m.

$$\frac{-\hbar^2}{2m}\frac{d^2\psi(x)}{dx^2} + V(x)\psi(x) = E\psi(x) \tag{2-10}$$

A classical-mechanical Hamiltonian can be defined for a particle of mass m moving in one dimension. This Hamiltonian, H, is equal of the total energy of the system's kinetic energy and potential energy and must be expressed as function of coordinates $(\mathrm{x}, \mathrm{y}, \mathrm{z})$and conjugate momenta, $(\mathrm{p_x}, \mathrm{p_y}, \mathrm{p_z})$ not velocities.

$$H = \frac{p^2 x}{2m} + V(x) \tag{2-11}$$

In quantum mechanics, every physical property has a corresponding quantum mechanical operator. The quantum mechanical operator for the Hamiltonian function is given as

$$\hat{H} = \hat{T} + \hat{V} = \frac{-\hbar^2}{2m}\frac{d^2}{dx^2} + V(x) \tag{2-12}$$

$\hat{T}\ and\ \hat{V}$ are the kinetic and potential energy quantum mechanical operators respectively. Quantum mechanics postulates that the measurement of a certain property be an eigenvalue of the operator corresponding to the operator of the physical property. For example:

$$\hat{H}\psi_i = E_i\psi_i \tag{2-13}$$

The wave function $\psi_i$is the eigenfunction and E_i is the eigenvalue of the Hamiltonian operator. In quantum mechanics, the only "allowed" energy values must be the eigenvalues of the Hamiltonian operator.[100]

The Schrödinger equation can be extended to a three-dimensional, multiple particle system. In this case, the kinetic energy will be the total of the individual kinetic energies of the individual particles.

$$\hat{T} = -\sum_{i=1}^{n} \frac{\hbar^2}{2m_i}\left(\frac{\partial^2}{\partial x_i^2} + \frac{\partial^2}{\partial y_i^2} + \frac{\partial^2}{\partial z_i^2}\right) \tag{2-14}$$

The potential energy is the sum of the electrostatic interaction among the particles.

$$V = \frac{1}{4\pi\varepsilon_0}\sum_{l}\sum_{b<a}\frac{q_a q_b}{r_{ab}} \tag{2-15}$$

ε_0 is the permittivity of free space, $q_a \; and \; q_b$ are the charges on the a^{th} and b^{th} particles separated by distance r_{ab}.

Electron Spin and Antisymmetric Properties

In addition to the orbital angular momentum, the electron also possesses a spin angular momentum or simply spin. This new property is a relativistic phenomenon and the lack of classical effect made it impossible to use macroscopic models to describe spin. The idea of nonrelativistic quantum mechanics treats spin as an additional hypothesis. In this case, the wave function also depends on the spin of the electron in addition to the cartesian coordinate.

$$\Psi(x, y, z, m_s) = \psi(x, y, z)\boldsymbol{g}(m_s) \tag{2-16}$$

where $\boldsymbol{g}(m_s)$ can either be of the spin eigenfunctions or a linear combination of the spin eigenfunctions with the eigenvalues of $+1/2$ or $-1/2$. Taking spin-orbit coupling into account not only changes the values of the energies that are obtained, but also the number of possible energy states is doubled. This can be as expressed as written below.

$$\hat{H}[\psi(x, y, z)g(m_s)] = g(m_s)\hat{H}\psi(x, y, z) = E[\psi(x, y, z)g(m_s)] \tag{2-17}$$

The spin creates a degeneracy as experienced in the hydrogen atom energy levels which is $2n^2$ rather than n^2. The uncertainty principle[101] prevents us from determining the exact paths taken by microscopic particles, resulting in indistinguishability of identical particles.
The indistinguishability of the electrons imposes a restriction to the wave function, such that the wave function must be antisymmetric with respect to the interchange of any two electrons.[101]

$$\psi(q_1, q_2, q_{3,}q_4 \dots \dots \dots, q_n) = -\psi(q_2, q_1, q_{4,}\, q_{3,} \dots \dots \dots, q_n) \qquad (2\text{-}18)$$

The Schrödinger equation cannot be separated for a system of interacting particles such as an atom or molecule. Hence the need for approximation methods to solve this deficiency. Approximation methods include: The Born-Oppenheimer approximation, Variational Method, Perturbation Theory, Density Functional Theory (DFT) and Hartree-Fock Self Consistent Field Theory (HF-SCF).

Approximation Methods

Born-Oppenheimer Approximation

The Born-Oppenheimer approximation was proposed by Max Born and his graduate student J. Robert Oppenheimer in 1927[102] and assumes that the nuclear and electronic motions are separable. Thus, the solution to the nuclear Schrödinger equation is therefore given as:

$$\widehat{H}_N\psi_N = U\psi_N \qquad (2\text{-}19)$$

The Born-Oppenheimer approximation considers the nuclei and the electrons as point masses[103] and disregarding relativistic interactions, the molecular Hamiltonian can be defined as:

$$\widehat{H} = -\frac{\hbar^2}{2}\sum_i \frac{1}{m_i}\nabla_i{}^2$$

$$-\frac{\hbar^2}{2m_e}\sum_\alpha \nabla_\alpha{}^2 + \sum_i\sum_{j>i}\frac{Z_i Z_j e^2}{r_{ij}} - \sum_i\sum_\alpha \frac{Z_1 e^2}{r_{\alpha i}} + \sum_\beta\sum_{\alpha>\beta}\frac{e^2}{4\pi\varepsilon_0 r_{\alpha\beta}} \quad (2\text{-}20)$$

where α and β refer to electrons i and j refer to nuclei. e is the charge on the proton and r is the distance between two particles. The first term is the kinetic energy of the nuclei, and the second term is the kinetic energy of the electrons. The third term is the electrostatic energy of repulsion of nuclei i and j, separated by a distance r_{ij}. The fourth term is the electrostatic energy between the electron α and nucleus i. The fifth term is the potential energy of the repulsions between electrons α and β. The molecular Hamiltonian operator for H_2 molecule is thus given as

$$\widehat{H} = -\frac{\hbar^2}{2m_p}\nabla_i{}^2 - \frac{\hbar^2}{2m_p}\nabla_j{}^2 - \frac{\hbar^2}{2m_e}\nabla_1{}^2$$

$$-\frac{\hbar^2}{2m_e}\nabla_2{}^2 + \frac{e^2}{4\pi\varepsilon_0}\left(\frac{1}{r_{ij}} - \frac{1}{r_{1i}} - \frac{1}{r_{1j}} - \frac{1}{r_{2i}} - \frac{1}{r_{2j}} + \frac{1}{r_{12}}\right) \quad (2\text{-}21)$$

The Schrödinger equation can then be written as

$$\widehat{H}\psi(q_\alpha, q_i) = E\psi(q_\alpha, q_i) \quad (2\text{-}22)$$

The approximation assumes that electrons move faster than nuclei with the same kinetic energy due to lighter mass. Therefore, the nuclei can be considered stationary with respect to the motion of the electrons. By parametrization of the nuclear positions, the kinetic energy term vanishes, and the Schrödinger equation for electronic motion is:

$$(\widehat{H}_{el} + V_{NN})\psi_{el} = U\psi_{el} \quad (2\text{-}23)$$

The electronic Hamiltonian $\hat{H}_{el}$ is given as

$$\hat{H}_{el} = \frac{\hbar^2}{2m_e}\sum_i {\nabla_i}^2 - \sum_i\sum_\alpha \frac{Z_i e^2}{r_{\alpha i}} + \sum_\beta\sum_{\alpha>\beta} \frac{e^2}{4\pi\varepsilon_0 r_{\alpha\beta}} \tag{2-24}$$

The nuclear repulsion term V_{NN} is given as

$$V_{NN} = \sum_i\sum_{j>i} \frac{Z_i Z_j e^2}{r_{ij}} \tag{2-25}$$

U is the electronic energy and also includes internuclear repulsion**,** V_{NN} is constant for a particular nuclear configuration and it is independent of electronic motion. The internuclear distance r_{ij} is fixed at a constant value, therefore the parameters of the electronic wave functions and energies depend on the nuclear coordinates.

$$\psi_{el} = \psi_{el,n}(q_\alpha, q_i) \tag{2-26}$$

$$U = U_n(q_n) \tag{2-27}$$

since V_{NN} is independent of electronic motion. Then, it can be removed from the Schrödinger equation to give:

$$\hat{H}_{el}\psi = E_{el}\psi_{el} \tag{2-28}$$

The total energy is the sum of both E_{el} and V_{NN}

$$U = V_{NN} + E_{el} \tag{2-29}$$

The value of U can be obtained using Equation 2-28 but V_{NN} can be calculated from Equation 2-25.

Hartree-Fock Self-Consistence Field Theory

The exact wavefunction for the hydrogen atom is known. However, for multi-electron systems, such as helium and lithium, the Hartree-Fock procedure is used to calculate the wave functions. This wave function may be calculated accurately by incorporating the interelectronic distance as a variable in the variational.

The Hamiltonian for an n-electron system is given as

$$\widehat{H} = -\frac{\hbar^2}{2m_e}\sum_{i=1}^{n}\nabla_i^{\,2} - \sum_{i=1}^{n}\frac{Ze^2}{r_i} + \sum_{i=1}^{n-1}\sum_{j=i+1}^{n}\frac{e^2}{r_{ij}} \qquad (2\text{-}30)$$

This ensures nucleus the is fixed at the coordinate origin. Therefore, only electronic motions contribute to the internal motion. The first summation includes the kinetic energy terms for n electrons. The second sum is the potential energy for attraction between the electrons and the nucleus of charge Ze . The last summation is the interelectronic repulsion term, and the restriction $j = i + 1$ avoids double counting of the same repulsions and excludes non- existent terms consisting of electron repulsion of itself. Ignoring the interelectronic repulsion, the Schrödinger equation can be separated into n one-electron equations like the solvable hydrogen atom equation. The zeroth order wave functions can be written as a product of one-electron spatial wave functions, f_i, called orbitals.

$$\psi^{(0)} = f_1(r_{1,}\theta_{1,}\phi_1)f_2(r_{2,}\theta_{2,}\phi_2)f_3(r_{3,}\theta_{3,}\phi_3)\ldots f_n(r_{n,}\theta_{n,}\phi_n) \qquad (2\text{-}31)$$

$$f = R_{nl}(r)Y_l^m(\theta,\phi) \qquad (2\text{-}32)$$

$R_{nl}(r)$ is known as the radial wave function and it is given by:

$$R_{nl}(r) = \left\{\frac{(n-l-1)!}{2n[n+1)!]}\right\}^{1/2}\left(\frac{2}{na_0}\right)^{l+3/2} r^l e^{-r/na_0} L_{n+1}^{2l+1}\left(\frac{2r}{na_0}\right) \qquad (2\text{-}33)$$

where n is the principal quantum number and l is the angular momentum quantum number. a_0 is the Bohr radius, and the L_{n+1}^{2l+1} are the associated Laguerre polynomials. The $Y_l^m(\theta,\phi)$ are the spherical harmonics.

$$Y_l^m(\theta,\phi) = \left|\frac{(2l+1)}{4\pi}\frac{(l-|m|)!}{l+|m|)!}\right|^{1/2} P_l^{|m|}(cos\theta)e^{im\phi} \tag{2-34}$$

m is the magnetic quantum number, with $|m| \leq l. P_l^{|m|}(cos\theta)$ are the associated Legendre polynomials.

$$P_l^{|m|}(cos\theta) = \frac{1}{2^l l!}(1-cos^2\theta)^{|m|/2}\frac{d^{l+|m|}}{d(cos\theta)^{l+|m|}}(cos^2\theta-1)^l \tag{2-35}$$

Equation 2-31 has a fundamental error, such that all orbitals use the same nuclear charge and does not account for shielding effects due to inner electrons. The approximations can be made more accurate by using different effective nuclear charges for different orbitals thus the shielding effect is considered. This is achieved using variational functions that are not restricted to any particular orbital.

$$\phi = g_1(r_{1,}\theta_{1,}\phi_1)g_2(r_{2,}\theta_{2,}\phi_2)g_3(r_{3,}\theta_{3,}\phi_3)\ldots g_n(r_{n,}\theta_{n,}\phi_n) \tag{2-36}$$

The functions $g_{1,}g_{2,}g_{3..,}g_{n,}$ are varied to minimize the variational integral given as:

$$E_1 \leq \frac{\int \emptyset^* H\widehat{\emptyset}d\tau}{\int \emptyset^*\emptyset d\tau} \tag{2-37}$$

E_1 is the ground state energy of the system. The Hartree-Fock Self Consistent Field method is used to calculate the $g_{i'_{s.}}$The first step in the Hartree-Fock procedure is to guess the product of the wave function[100]

$$\phi = s_1(r_{1,}\theta_{1,}\phi_1)s_2(r_{2,}\theta_{2,}\phi_2)s_3(r_{3,}\theta_{3,}\phi_3)\ldots s_n(r_{n,}\theta_{n,}\phi_n) \tag{2-38}$$

where the $s_i{}'$s are the products of the normalized wave function and the spherical harmonics. In this approximation, the electrostatic electron-electron repulsion term is averaged, meaning that the first electron experiences a field created by averaging out the other electrons. Coulombs law defined the potential energies that exist between charges q_1 and q_2 (in atomic units).

$$V_{12} = \frac{q_1\, q_2}{r_{12}} \tag{2-39}$$

If Electron 2 is averaged out as a continuous charge distribution of ρ^v , and considering the infinitesimal charge $\rho_2 dv_2$ in an infinitesimal volume dv_2. The average interaction between q_1 and the infinitesimal elements of charge q_2 is given as

$$V_{12} = \frac{q_1}{4\pi\varepsilon_0}\int \frac{\rho_2}{r_{12}} dv_2 \tag{2-40}$$

where r_{12} is the distance between the first electron with charge q_1 and the charge distribution density ρ_2. If the probability density of Electron 2 is$|s_2|^2$ then $\rho_2 = -e|s_2|^2$.

$$V_{12} = \frac{e^2}{4\pi\varepsilon_0}\int \frac{|s_2|^2}{r_{12}} dv_2 \tag{2-41}$$

The summation of the interactions with the other electrons is

$$V_{12} + V_{13} + V_{14} + \cdots V_{1n} = \sum_{j=2}^{n} \frac{e^2}{4\pi\varepsilon_0}\int \frac{\left|s_j\right|^2}{r_{1j}} dv_j \tag{2-42}$$

The potential energy between Electron 1 and the nucleus and the other electrons is given as

$$V\left(r_{1,}\theta_{1,}\emptyset_1\right) = \sum_{j=2}^{n} \frac{e^2}{4\pi\varepsilon_0}\int \frac{\left|s_j\right|^2}{r_{1j}} dv_j - \frac{Ze^2}{4\pi\varepsilon_0 r_1} \tag{2-43}$$

Averaging $V(r_{1,}\theta_{1,}\emptyset_1)$ over the angles θ and $\emptyset$ is necessary because the approximation uses the result that the effective potential acting on an electron is a function of r only.

$$V_1(r_1) = \frac{\int_0^{2\pi}\int_0^{2\pi} V_1(r_1,\theta_1,\phi_1) sin\theta d\theta_1 d\phi_1}{\int_0^{2\pi}\int_0^{\pi} sin\theta d\theta d\phi} \tag{2-44}$$

Inputting $V_1(r_1)$ into the one-electron Schrödinger equation as the potential energy term, we have:

$$\left[\frac{\hbar^2}{2m_e}\nabla_1{}^2 + V_1(r_1)\right] t_1(1) = \varepsilon_1 t_1(1) \tag{2-45}$$

We have successfully obtained an improved Schrödinger equation with wave functions t_1 and orbital energy ε_1. To ensure that input and output wave functions match, the procedure is repeated iteratively until they are self-consistent. The orbitals obtained from this procedure are known as the Hartree-Fock orbitals. The approximation to the exact wave functions should consider the Pauli's exclusion principle and must be antisymmetric with respect to the interchange of electrons. Therefore, we can include anti-symmetrical spin-orbitals to the properties of the electrons. The differential equation for the Hartree-Fock calculation showing the effective Hamiltonian operator also known as the Fock operator, is given below.

$$\hat{F}u_i = \mathcal{E}_i u_i \,, \qquad i = 1,2 \ldots n \tag{2-46}$$

where $\hat{F}$ is the Fock operator, u_i is the spin orbital corresponding to the orbital energy $\mathcal{E}_i$. The antisymmetric wave function is satisfied by the Slater determinant.[104] The elements in the column involve the same spin orbital while the elements in the same row involve the same electron. The ground state wave function for helium can be written as a linear combination to give the antisymmetric wave function.

$$1s(1)1s(2)\ \frac{1}{\sqrt{2}}[\alpha(1)\beta(2)-\beta(1)\alpha(2)]=\frac{1}{\sqrt{2}}\begin{vmatrix}1s(1)\alpha(1) & 1s(1)\beta(1)\\ 1s(2)\alpha(2) & 1s(2)\beta(2)\end{vmatrix} \quad (2\text{-}47)$$

The wavefunction of a Slater determinant is known as a determinantal wave function. The determinantal wave function for N-electron is given below

$$\Psi=\begin{pmatrix}a_1(1) & \cdots & a_N(1)\\ \vdots & \ddots & \vdots\\ a_1(N) & \cdots & a_N(N)\end{pmatrix} \quad (2\text{-}48)$$

where a_n is orthonormal to spin orbitals. The development of Hartree-Fock SCF has provided solutions to closed-shell and open shell systems. A restricted or unrestricted method can be used in both open shell and closed shell systems.[105] In a closed-shell system, the restricted Hartree-Fock (RHF) places paired electrons that are opposite in spin in a spatial orbital function. Like RHF, the restricted open shell also places paired electrons that are opposite to the same spatial orbital. The unrestricted Hartree-Fock (UHF) method allows paired electrons to occupy different spatial orbitals.

$$E=\langle S|\widehat{H}_{el}|S\rangle=2\sum_{i=1}^{1/2}\langle\phi_1(1)|f_i|\phi_1(1)\rangle+\sum_{j=1}^{n/2}\sum_{i=1}^{n/2}\left(2J_{ij}-K_{ij}\right) \quad (2\text{-}49)$$

where the ϕ_i are the $n/2$ spatial orbitals for n electron and space is the Slater determinant Hartree-Fock wave functions. The molecular electronic Hamiltonian is

$$\widehat{H}_{el}=\sum_{i=1}^{n}f_i+\sum_{i=1}^{n-1}\sum_{j>i}\hat{g}_{ij} \quad (2\text{-}50)$$

$\hat{g}_{ij}$ and f_i are the two-electron operators and one-electron operators, respectively, which is defined as

$$\hat{g}_{ij=\frac{1}{r_{ij}}} \tag{2-51}$$

$$\hat{f}_i = -\frac{1}{2}\nabla_i{}^2 - \sum_{\alpha}\frac{Z_a}{r_{ia}} \tag{2-52}$$

The Hartree-Fock molecular energy of a closed shell diatomic or polyatomic molecule

$$E_H = \langle S|H_{el} + V_{NN}|S\rangle \tag{2-53}$$

$$E_{HF} = 2\sum_{i=1}^{n/2} H_{ii}^{core} + \sum_{j=1}^{n/2}\sum_{i=1}^{n/2}\left(2J_{ij} - K_{ij}\right) + V_{NN} \tag{2-54}$$

H_{ii}^{core} is a known one-electron core hamiltonian

$$H_{ii}^{core} = \langle\phi_i(1)\left|\hat{H}^{core}(1)\right|\phi_i(1)\rangle = \langle\phi_i(1)\left|-\frac{1}{2}\nabla_i^2 - \sum_{\alpha}\frac{Z_\alpha}{r_{i\alpha}}\right|\phi_i(1)\rangle \tag{2-55}$$

where

$$J_{ij} = \langle\phi_i(1)\phi_j(2)|1/r_{12}|\phi_i(1)\phi_j(2)\rangle \tag{2-56}$$

$$K_{ij} = \langle\phi_i(1)\phi_j(2)|1/r_{12}|\phi_i(1)\phi_j(2)\rangle \tag{2-57}$$

$\hat{H}^{core}(1)$ is the kinetic energy operator for electron 1. The coulomb and exchange integrals are represented by J_{ij} and K_{ij} respectively and are integrated over spatial coordinates for electrons 1 and 2. One important characteristic of the Hartree-Fock method is that it helps to find molecular orbitals that minimize the variation integral E_{HF}.[105] The orbitals are assumed to be normalized and orthogonal. Equation 2-58 satisfies these conditions:

$$\hat{F}(1)\phi_i(1) = \mathcal{E}_i\phi_i(1) \tag{2-58}$$

where $\mathcal{E}_i$ is the orbital energy and the Hartree-Fock operator is given as:

$$\hat{F}(1) = \hat{H}^{core}(1) + \sum_{j=1}^{n/2}\left[2j_j(1) - K_j(1)\right] \tag{2-59}$$

The coulomb operator and exchange operator that include an arbitrary function f are given below:

$$\hat{J}_j(1)f(1) = f(1)\int \left|\phi_j(2)\right|^2 \frac{1}{r_{12}} d \tag{2-60}$$

$$\hat{K}_j(1)f(1) = \phi_j(1)\int \frac{\phi_j^*(2)f(2)}{r_{12}} dv_2 \tag{2-61}$$

By multiplying the Equation 2-58 by ϕ_i^* and integrating over all space we can calculate the orbital energy.

$$\mathcal{E}_i = \langle\phi_i(1)\left|\hat{H}^{core}\right|\phi_i(1)\rangle + \tag{2-62}$$

$$\sum_j \left[2\langle\phi_i(1)\left|\hat{j}_j(1)\right|\phi_i(1)\rangle - \langle\phi_i(1)\left|\hat{K}_j(1)\right|\phi_i(1)\rangle\right]$$

which simplifies to

$$\mathcal{E}_i = H_{ii}^{core} + \sum_{j=1}^{n/2}(2j_{ij} - K_{ij}) \tag{2-63}$$

Summing Equation 2-62 over $n/2$ occupied orbitals gives

$$\sum_{i=1}^{n/2}\mathcal{E}_i = \sum_{i=1}^{n/2}\hat{H}_{ii}^{core} + \sum_{j=1}^{n/2}\sum_{i=1}^{n/2}(2J_{ij} - K_{ij}) \tag{2-64}$$

The Hartree-Fock energy is obtained by solving $\sum H_{ii}^{core}$

$$E_{HF} = 2\sum_{i=1}^{n/2} \mathcal{E}_i - \sum_{i=1}^{n/2}\sum_{i=1}^{n/2}\left(2J_{ij} - K_{ij}\right) + V_{NN} \tag{2-65}$$

Hartree-Fock-Roothaan Equations

Roothaan proposed that the Hartree-Fock spatial orbitals could be represented by linear combinations of one-electron basis functions.[106-107]

$$\phi_i = \sum_{j=1}^{a} c_{ij}\chi_j \tag{2-66}$$

where χ_j is the set of one-electron basis functions and c_{ij} are the coefficients of expansion. a is the number of basis functions and should be as large as possible to minimize the error.

Substituting the expression for ϕ_i in Equation 2-58 results to:

$$\sum_j C_{ji}\hat{F}\chi_j = \mathcal{E}_i \sum_j C_{ji}\,\chi_j \tag{2-67}$$

Multiplying Equation 2-66 by χ_p and integrating gives a set of linear homogenous equations that describe a molecular orbital.

$$\sum_{j=1}^{a} C_{si}\left(F_{pj} - \mathcal{E}_i S_{pj}\right) = 0 \quad p = 1, 2, \ldots, a \tag{2-68}$$

where

$$F_{pj} = \langle\chi_p|\hat{F}|\chi_j\rangle \tag{2-69}$$

$$S_{pj=}\langle\chi_p|\chi_j\rangle \tag{2-70}$$

For a non-trivial solution:

$$det = (F_{pj} - \mathcal{E}_i S_{pj}) = 0 \tag{2-71}$$

The root of this equation provides the orbital energies. The Hartree-Fock-SCF wave functions tend to average out electron-electron interactions.

Electrons do repel each other and therefore, there exists a space where the probability of finding an electron is small. This is known as a coulomb hole, which is the result of the correlated electron motions. So, the wave function can be corrected for instantaneous electron correlation

$$E_{corr} = CE = E_{exact} - E_{HF} \tag{2-72}$$

Density Functional Theory

The probability of finding an electron in terms of spatial and spin coordinates in a given volume element is given as

$$\rho_{(x,y,z)} = \left|\psi(x_{1,}\, y_{1,}\, z_1, \dots, x_{n,}\ y_{n,}\ z_{n\,}, m_{s1,\dots,} m_{sn}\right|^2 d_{x1} d_{y1} d_{z1} \dots d_{xn} d_{yn} d_{zn} \tag{2-73}$$

The distribution function above describes the probability of finding n electrons with spin m_{sn} in the volume element $d_{x1} d_{y1} d_{z1}$. Ignoring electron spin, the summation of the probability over all possible states for all the electrons gives:

$$\sum_{m_{s1}} \dots \sum_{m_{sn}} |\psi|^2 d_{x1} d_{y1} d_{z1} \dots d_{xn} d_{yn} d_{zn} \tag{2-74}$$

Ignoring the location of all other electrons, the probability density of locating an electron at coordinate x, y, z can be determined by integrating over the coordinates of all other electrons.

$$\rho_{(x,y,z)} = n \sum_{m_s} \int \dots \int \left|\psi(x, y, z, x_{2,\dots}\ z_{n\,}, m_{s1,\dots,} m_{sn}\right|^2 d_{x2} \dots d_{zn} \tag{2-75}$$

Representing this in vector notation gives

$$\rho_{(r)} = n \sum_{m_s} \int \dots \int \left|\psi(r, r_{2,}, \dots, r_{n,}\ m_{s1,\dots,} m_{sn}\right|^2 dr_2 \dots dr_n \tag{2-76}$$

The average for an n-electron molecule is given as:

$$\langle \psi \left| \sum_{i=1}^{n} f(r_i) \right| \psi \rangle = \int \psi^* \sum_{i=1}^{n} f(r_i) \psi d\tau = \sum_{i=1}^{n} \psi^2 f(r_i) d\tau \tag{2-77}$$

Since electrons are indistinguishable, the value of the last summation can be simplified for n electrons

$$\langle \psi \left| \sum_{i=1}^{n} f(r_i) \right| \psi \rangle = \int n|\psi|^2 f(r_i) d\tau \tag{2-78}$$

The probability density can be simplified to

$$\int \psi^* \sum_{i=1}^{n} f(r_i) \varphi d\tau = \int \rho(r) f(r) d\tau \tag{2-79}$$

In 1964, Pierre Hohenberg and Walter Kohn proposed that electron density, rather than the wave function provides all the information for a many electron system and that the molecular energies can be determined completely by the ground state electron probability density $\rho_0(x, y, z)$.[108] For example, there are four coordinates for each single electron if the spin is included. This makes it complicated to calculate the energy and other properties for many electron molecules using the wave functions. A substitute for the wavefunction is possible, which has fewer variables but can still provide all the information about the system. According to Hohenberg and Kohn the ground state electronic energy E_0, is directly proportional to the probability density and given as

$$E_0 = E_0[\rho_0] \tag{2-80}$$

The electronic Hamiltonian in atomic units can be written as

$$\widehat{H} = -\frac{1}{2} \sum_{i=1}^{n} {\nabla_i}^2 + \sum_{i=1}^{n} v(r_i) + \sum_{i} \sum_{j>i} \frac{1}{r_{ij}} \tag{2-81}$$

$$v(r_i) = -\sum_a \frac{Z_a}{r_{ia}} \tag{2-82}$$

The term $v(r_i)$ is the potential energy for the interaction between electron i and the nuclei. The wave function and the energy of the system are determined as a solution to the Schrödinger equation having known the external potential and the number of electrons.

The Hohenberg-Kohn theorem states that the external potential and the number of electrons is given by the ground state electron probability density. Hence the electron density gives the wave functions and energy of the system under consideration. The electron density determines the number of electrons by

$$\int \rho_0(r)dr = n \tag{2-83}$$

From the above, it suggests that the ground state electronic energy is a functional of the electron probability density which can be represented by

$$E_0 = E_v = [\rho_0]$$

The ground state energy is written as;

$$E_0 = E_v[\rho_0] = \bar{T}[\rho_0] + \bar{V}_{Ne}[\rho_0] + \bar{V}_{ee}[\rho_0] \tag{2-85}$$

The sum of the average kinetic energy term $\bar{T}$, average electron-nuclear attraction term, $\bar{V}_{Ne}$, and the average electron-electron repulsion term, $\bar{V}_{ee}$, is the is energy of the system.

$$\bar{V}_{Ne} = \langle \varphi_0 \left| \sum_{i=1}^{n} v(ri) \right| \varphi_0 \rangle = \int \rho(r)v(r)d\tau \tag{2-86}$$

Where the unknowns in Equation 2-85 are the $\bar{V}_{Ne}[\rho_0]$ and $\bar{V}_{ee}[\rho_0]$ and are independent of the external potential.

Kohn- Sham Method

The Hohenberg-Kohn theorem has a major disadvantage such that it lacks information regarding the evaluation of the ground state energy term from the electron density. Thus, in 1965 Kohn and Sham proposed a method to calculate the ρ_0 and evaluating E_0 from ρ_0.[109] The method uses a fictitious non-interacting system of n electrons. It also concluded that all non-interacting electrons experience the same external potential energy function $v_s(ri)$ such that the electron probability density of the reference system $\rho_s(r)$ is equal to the ground state electron density of the molecule $\rho_0(r)$. The Hamiltonian for a reference system is equal to

$$\hat{H} = \sum_{i=1}^{n}\left[-\frac{1}{2}\nabla^2 i + v_s(ri)\right] = \sum_{i=l}^{n}\hat{h}_i{}^{ks} \tag{2-87}$$

The reference system is related to the real molecule by including an extra term such that:

$$\hat{H} = \hat{T} + \sum_i v(r_i) + \lambda\hat{V}_{ee} \tag{2-88}$$

where the value of λ ranges from 0 (the non-interelectronic repulsions that is the reference system) to 1 (the real system).

The Slater determinant of Kohn-Sham spin-orbitals is given as:

$$\varphi_{s,0} = \left|\left|u_1{}^{ks}\, u_2{}^{ks} \ldots u_n{}^{ks}\right|\right| \tag{2-89}$$

$$u_i{}^{ks} = \theta_i{}^{ks}(ri)\sigma i \tag{2-90}$$

The spatial function $\theta_i{}^{ks}$ is the eigenfunction of the one-electron Kohn-Sham Hamiltonian.

$$\hat{h}_i{}^{ks}\theta i^{ks} = \hat{\varepsilon}_i{}^{ks}\theta i^{ks} \tag{2-91}$$

Kohn and Sham modified Equation 2-86 and defined the new terms as follows.

$$E_0 = E_v[\rho_0] = \int \rho_0(r)v(r)dr + \bar{T}_s[\,\rho_0] + \frac{1}{2}\iint \frac{\rho_0(r_1)\rho_0(r_2)}{r_{12}} dr_1 dr_2 + \Delta\bar{T}[\rho_0] + \Delta\bar{V}_{ee}[\rho_0] \tag{2-92}$$

$$\Delta\bar{T}[\rho_0] = \Delta\bar{T}[\rho_0] - \Delta\bar{T}_s[\rho_0] \tag{2-93}$$

$$\Delta\bar{V}_{ee}[\rho_0] = \bar{V}_{ee}[\rho_0] - \frac{1}{2}\iint \frac{\rho_0(r_1)\rho_0(r_2)}{r_{12}} dr_1 dr_2 \tag{2-94}$$

The double integral on the right of the expression represents the interelectronic repulsion energy for electrons smeared out as a continuous charge distribution with density ρ . Combining Equations 2-93, 2-94, and 2-86 gives:

$$E_v[\rho_0] = \int \rho_0(r)v(r)dr + \bar{T}_s[\,\rho_0] + \Delta\bar{T}_s[\rho_0] + \frac{1}{2}\iint \frac{\rho_0(r_1)\rho_0(r_2)}{r_{12}} dr_1 dr_2 + \Delta\bar{V}_{ee}[\rho_0] \tag{2-95}$$

where the unknowns ΔT and ΔV_{ee} are the summation which are defined as the correlation energy functional given as:

$$E_{xc}[\rho_0] = \Delta\bar{T}[\rho_0] + \Delta\bar{V}_{ee}[\rho_0] \tag{2-96}$$

In Equation 2-93, the terms are separated so that the essential contribution from E_0 are the first three terms, and are calculated from a known electron density, and the smallest contribution from the unknown functional $E_{xc}[\rho_0]$. The electronic kinetic energy and the external potential energy can be substituted into the Equation 2-95 to yield

$$E_0 = -\sum_a Z_a \int \frac{\rho_{0(r_1)}}{r_{1a}} dr_1 - \tag{2-97}$$

$$\frac{1}{2}\sum_{i=1}^{n} \langle \theta_i{}^{ks}(1) \left| \nabla_1{}^2 \right| \theta_i{}^{ks}(1) \rangle + \frac{1}{2} \iint \frac{\rho_0(r_1)\rho_0(r_2)}{r_{12}} dr_1 dr_2 + E_{xc}[\rho_0]$$

Recall that the reference system was chosen as $\rho_0 = \rho_s$ the ground state electron density can be calculated from

$$\rho_0 = \rho_s = \sum_{i=1}^{n} \left| \theta_i{}^{ks} \right|^2 \tag{2-98}$$

where $\theta_i{}^{ks}$ is known as the spatial part of the anti-symmetric wave function. So, the ground state electronic energy E_0 can be calculated from (KS) orbitals $\theta_i{}^{ks}$ and a good approximation $E_{xc}[\rho_0]$.

The Kohn-Sham orbitals satisfy the equation;

$$\left[-\frac{1}{2}\nabla_1{}^2 - \sum_\alpha \frac{Z_\alpha}{r_{12}} + \int \frac{\rho(r_2}{r_{12}} dr_2 + v_{xc}(1) \right] \theta_i{}^{ks}(1) = \varepsilon_i{}^{ks} \theta_i{}^{ks}(1) \tag{2-99}$$

v_{xc} is the exchange correlation potential and it is defined as the functional derivative of the exchange correlation potential.

$$v_{xc}(r) = \frac{\delta E_{xc}[\rho(r)]}{\delta \rho(r)} \tag{2-100}$$

B3LYP Functional

The sum of the exchange functional E_x and correlation-energy functional E_c gives the exchange correlation functional E_{xc}.

$$E_{xc} = E_x + E_c \tag{2-101}$$

E_x can be derived from the terms in Equation 2-63 that involve the exchange integral K_{ij} defined in Equation 2-56 by replacing the Hartree-Fock orbitals with Kohn-Sham orbitals.

$$E_x = -\frac{1}{4}\sum_{i=1}^{n}\sum_{j=1}^{n}\langle {\theta_i}^{ks}(1){\theta_j}^{ks}(2)\left|\frac{1}{r_{12}}\right|{\theta_j}^{ks}(1){\theta_i}^{ks}(2)\rangle \qquad (2\text{-}102)$$

The constant $1/4$ accounts for the double sum of n^n electrons instead of $n/2$ orbitals in Equation 2-65. The correlation energy functional can be calculated from the subtraction of E_x and E_{xc}. In other to obtain a more accurate result, approximating both E_x and E_c using a model may be necessary. This results in the exchange -correlation functional:

$$E_x^{LDA}[\rho] = \int \rho(r)\varepsilon_{xc}(\rho)dr \qquad (2\text{-}103)$$

The exchange plus correlation energy $\varepsilon_{xc}(\rho)$ is an assumption that the electron is surrounded by a homogenous electron gas of electron of electron density ρ. The Local Spin Density Approximation (LSDA) model rather than LDA is most suitable for open shell systems because it allows electron pairs to have different spatial KS orbitals, thus the LSDA is analogous to the UHF method in which the different Hartree-Fock orbitals for electrons have different spins.

To improve on the LDA and LSDA models, the electron density dependence on position must be specified. The introduction of the generalized-gradient approximation (GGA) incorporates this dependency by including the gradients of the electron densities ρ^α and ρ^β of the paired electrons.

$$E_{xc}^{GGA}[\rho] = \int f(\rho^\alpha(r),(\rho^\beta(r),\nabla(\rho^\alpha(r),\nabla\left(\rho^\beta(r)\right)dr \qquad (2\text{-}104)$$

where f is a function and it depends on the spin densities and their gradients, and ∇ is the first order differential operator. A gradient correction to the E_x^{LSDA} was described by Becke's 1988 exchange functional and it is given as[110]

$$E_x^{B88} = E_x^{LSDA} -$$

$$b \sum_{\sigma=\alpha,\beta} \int \frac{(\rho^\sigma)^{4/3} \chi_\sigma^2}{1 + 6b\chi_\sigma \ln[\chi_\sigma + (\chi_\sigma^2 + 1)^{1/2}]} dr = E_x^{LSDA} + \Delta E_x^{B88} \quad (2\text{-}105)$$

b is an empirical parameter, χ_σ is equal to $|\nabla\rho^\sigma|/(\rho^\sigma)^{4/3}$ and E_x^{LDA} is given as

$$E_x^{LSDA} = -\frac{3}{4}\left(\frac{6}{\pi}\right)^{1/3} \int [(\rho^\alpha)^{4/3} + (\rho^\beta)^{4/3}] dr \quad (2\text{-}106)$$

Hybrid exchange-correlation functionals are now being used. The first hybrid exchange-correlation functional B3PW91 was proposed by Becke; it included Equation 2-101, the GGA exchange and correlation functionals.[111] The hybrid functional was named after Becke including the three parameters named as Becke3LYP or B3LYP and it is defined as:[112-113]

$$E_{xc}^{B3LYP} = (1 - a_0 - a_x)E_x^{LSDA} + a_0 E_x{}^{HF} + a_x E_x{}^{B88} + (1 - a_c)E_c^{VWN} + a_c E_c{}^{LYP} \quad (2\text{-}107)$$

where a_c, a_x and a_0 are parameters, $E_c{}^{LYP}$ represent GGA correlation functional developed by Lee et al.[18] E_c^{VWN}represents LSDA correlation developed by Vosko, *et al*.[114]

Basis Sets

Basis sets, as used in computational chemistry, refer to a sets of nonorthogonal functions called atomic orbitals which are used to build molecular orbitals. Thus, are said to be centered on atoms, although a few functions may be centered in bonds and lone pairs. A linear combination of Slater type orbitals (STOs) are used to represent atomic orbitals. The STOs shared some

similarities with the eigenfunctions of the hydrogen atoms. The general definition for a normalized STO for an atom of radius r in a linear molecule is given as:

$$S_{nlm}^{\zeta}(r,\theta,\phi) = \frac{(2\zeta/a_0)^{n+1/2}}{[(2n)!]^{1/2}} r^{n-1} e^{\zeta r/a_0} Y_l^m(\theta,\phi) \tag{2-108}$$

In the equation above the fractional is the normalization factor, $Y_l^m(\theta,\phi)$ is the spherical harmonic which describes the shape of orbital and takes the form $[(Y_l^m)^* \pm Y_l^m],/2^{1/2}$ for a nonlinear molecule to form cartesian orbitals. ζ is the orbital exponent which can only be a positive value. The exponential term controls the size of the orbital, where a large zeta gives a small dense function and a small zeta gives a large diffuse function. For polyatomic molecules, the calculations using STO basis functions usually results in a multi-center integral which is time consuming even for small molecules and cannot be performed efficiently. The Gaussian-type functions (GTF) were proposed by Boys in order to save computational time.[115] The Gaussian is centered on atom α with exponent α is

$$g_{ijk} = N x_a^i y_a^i z_a^i e^{-\alpha r_a^2} \tag{2-109}$$

where N is the normalization constant and it is equal to

$$N = \left(\frac{2\alpha}{\pi}\right)^{3/4} \left[\frac{(8\alpha)^{i+j+k} i!\, j!\, k!}{(2i)!\,(2j)!\,(2k)!}\right]^{1/2} \tag{2-110}$$

The sum of i, j, and k equals the angular momentum. The s-type Gaussian is given $i + j + k = 0$, p-type Gaussian as $i + j + k = 1$ and d-type as $i + j + k = 2$. Unlike STOs, GTOs do not represent hydrogen-like atoms due to the square of the radius in the exponential term. This usually results in the loss of the cusp at $r = 0$ and decays rapidly as r becomes larger. A linear combination of primitive Gaussian functions g_u that closely resembles a corresponding STO can be used to proffer the solution to the problem.

$$\chi_r = \sum_u d_{ur}\, g_u \tag{2-111}$$

d_{ur} is the contraction coefficient which is held constant throughout the calculation. χ_r is known as the contracted GTFs (CGTFs) and are even more efficient than STOs essentially because the product of two Gaussian functions at different centers is equal to a single Gaussian function at a new center. Many basis sets are composed of GTOs. The most basic and smallest are called minimal basis sets, which ensures that a single basis function is used for each atomic orbital. Double zeta (DZ), triple zeta (TZ), and quadruple zeta (QZ) bases use two, three and four basis functions with different orbital exponents for each AO, respectively. When the number of basis functions that describe an atomic orbital is increased, it allows more flexibility in the size of the orbital when other atoms approach.

Extended basis sets such as split-valence, polarized sets, diffuse sets, correlation consistent sets, and augmented sets are used to providing better accuracy in calculations. A split-valence basis set can be used to split inner and outer shell AOs. In this case each inner-shell AO is represented by a minimal basis set and each outer-shell AO is represented by two (valence double zeta:VDZ) or more basis functions (e.g VTZ, VQZ, etc). This is particularly useful because most chemical reactions occur between the valence electrons.

Polarized sets are used to add basis functions of higher momentum than that of ground state valence shell since chemical bonding in molecules results in anisotropic distribution of electrons that cannot be included by simply changing orbital exponents. Diffuse sets are used to describe orbitals that are far from the nucleus to account for weak anions, Rydberg states and van der Waals interactions. Augmented basis functions add one set of diffuse functions to the core valence/valence electron to give the aug-cc-pVXZ where X=(D, T,Z).

A contracted Gaussian type basis set known as a Pople basis set was developed by John Pople and coworkers to mimic the appearance of STOs.[116] The minimal basis is represented as STO-nG in which each AO is represented by the *n* primitive Gaussian functions. The Pople split-valence basis set takes the form k-nlm (idf, jpd) or nlm++G** where k, l, m, n are primitive GTFs for core, inner valence, medium valence and outer electrons, respectively. One asterisk indicates one set of five 3d polarization functions added to all non-hydrogen atoms, and two asterisks indicate an extra set of three 2p polarization functions added to hydrogen atoms. The idf in parentheses signifies *i* set of d-type and one set of *f*-type polarization functions added to non-hydrogen atoms, and the additional jpd term signifies *j* set of *p*-type and one set of *d*-type polarization functions added to hydrogen atoms. One positive sign denotes one set of *p*-type diffuse functions added to non-hydrogen atoms, and two positive signs denote a supplemental *s*-type diffuse function added to hydrogen atoms.

Correlation consistent basis set were proposed by Thomas Dunning and coworkers to recover the correlation energy of valence electrons.[117] Thus, they are built up by adding shells of functions to a core set of atomic Hartree-Fock functions. This results in very similar contributions to the amount of correlation energy from each of the function in the shells for an atomic calculation. In Dunning's work, correlation consistent polarized valence sets cc-pVXZ are built from X-zeta basis functions where X may be D, T Q, 5, 6, 7, etc.).[117-121] For example, cc-pVDZ consists of 3s2p1d. cc-pVTZ consists of 4s3p2d1f and cc-pVQZ would be 5s4p3d2f1g. Dunning's basis set were optimized using higher order correlated methods as opposed to Pople basis set which were optimized using HF calculations of atoms and small molecules. In addition, there is a systematic convergence to the complete basis set (CBS) limit, where the multi-electron basis is infinitely expanded and $X = \infty$.[122]

Extrapolation of Basis Sets

Calculations involving electronic structure are limited by slow convergence of correlated electrons. Complete basis set methods that extrapolate to a complete one-electron basis set for a given level of electron correlation or to the limit of complete interaction will be quite valuable in mitigating the problem of the slow convergence.

Halkier *et al.* and Martin[123-124] presented a practical method for the extrapolation of basis sets. A very accurate result was observed for small molecules by extrapolating from very large basis sets. They developed Equation 2-113 that extrapolates single point energies to the CBS limit using HF level theory.[121] Comparing the property value calculated at the CBS limit to the experimental value helps to determine the accuracy of any theoretical method.[125]

$$E_1(x) = E_{CBS} + \frac{B}{\left(x + \frac{1}{2}\right)^4} \tag{2-112}$$

Feller[126] introduced an exponential form of the CBS limit extrapolation which has three parameters and thus can be used for three energy calculations.

$$E_2(x) = E_{CBS} + Be^{-\alpha n} \tag{2-113}$$

In both Equation 2-113 and 2-114, E_{CBS} is the energy at the basis set limit, B and is a parameter and x is the number of the basis set limit, the value of x is 2, 3 , 4 etc. for cc-pVDZ, cc-pVTZ , cc-pVQZ respectively and reaches the CBS limit at x=∞

CHAPTER 3. RESULTS AND DISCUSSION

Computational Details

Ab initio calculations were performed using NWChem 6.8.1[127] software from the Molecular Sciences Laboratory Software group of Pacific Northwest National Laboratory on a Dell PowerEdge R730 server with 192 GB of memory and 12 TB of disk. Pictorial representations of the molecules were generated with the WebMO 17.0.012e interface.[1258] Basis set extrapolation calculations were performed with the online basis extrapolation calculator[129] and graphs were made with Curve Expert Professional 2.6.5[130] Optimized geometries were calculated using Hartree-Fock (HF) and Density Functional Theory (DFT) in conjunction with the Pople 6-31G and 6-31G(d) basis sets, correlation consistent polarized valence-only basis sets (cc-pVXZ; X=D, T, Q).

Basis set extrapolation methods uses optimized geometry energy calculations from Hartree-Fock and Density Functional Theories in conjunction with Dunning's cc-pVXZ (X=D, T, Q) basis sets. Geometry optimization at the quadruple-zeta basis level were difficult to obtain given the time frame, thus only single point molecular energy calculations were done at the quadruple-zeta basis level using double-zeta optimized geometries.

In view of the error expected from the calculations expected from molecular energy calculations other than geometry optimization, basis set extrapolations were also performed at only double-zeta (D) and triple-zeta (Z) to compensate for the error, which may be obtained from combining geometry optimization with single point molecular energy calculations. The complete basis set extrapolation limit curves for each molecule are given in appendix B, figures 23-38.

Discussion of Results

Melatonin has been identified as an antioxidant and several reaction paths have been identified. Experimental data are limited in providing accurate description of the reaction mechanisms thus, computational study is used in this research to give insight into the antioxidant activity of melatonin. The stability of the intermediate formed during the partial oxidation of melatonin can provide information about the antioxidant activity of melatonin. In addition, *in vivo* spin trapping of the radical by melatonin and its oxidation products can be determined.

Geometry optimizations of melatonin and its partial oxidation products: 2-OH-MLT, 4-OH-MLT and 6-OH-MLT were performed to determine the energies at the HF and DFT/B3LYP levels of theory. From our results, the energy data obtained for DFT is lower than HF at all basis sets. This supports a well-known fact that DFT is a more reliable method for the computation of molecular energies, geometry optimization, vibrational frequency, and molecular structures.[131]

The total energy was obtained by the sum of electronic energies obtained from the geometry optimization and the Zero Point Energy (ZPE) from frequency calculations. This total energy is required to compute the enthalpy of our reactions.

Tables 1 and 2 show the enthalpy of reaction of three oxidation products, 2-OH-MLT, 4-OH-MLT and 6-OH-MLT formed during the partial oxidation of melatonin with hydroxyl radicals. The results indicate that the reaction is exothermic for all the three paths. Clearly, the position of the hydroxyl group contributes to the stability of the oxidation products.

According to Galano[132], the reaction is expected to be exothermic and this research supports Galano's findings. Thermodynamically, the heat of reactions obtained from DFT calculations are lower than those obtained from HF calculations for all basis sets and at the CBS limit.

However, a similar trend is observed from both calculations: the heat of reaction for 2-OH-MLT path appears to be much lower than for both 4-OH-MLT and 6-OH-MLT paths indicating a more favorable path towards the formation of the 2-OH-MLT. Furthermore, electronic energies obtained from the optimization of geometry at all levels of theory indicate very low energy of the oxidation products compared to parent melatonin with 2-OH-MLT being the lowest. This observation is acceptable because the addition of the hydroxyl group improves the stability of molecules by donating an electron to the ring making it more stable. Thus, in the case of melatonin, we observed a much more stable oxidation product.

As stated earlier, the electronic energy of the 2-OH-MLT appears to be lower than the other oxidation products, this observation can be supported from the position of the phenol group. For 2-OH-MLT, the hydroxyl group is located on position 2 which favors the delocalization of electrons because it lies between a double bond and a lone-pair of electrons of nitrogen. Besides, the delocalization of electrons, 2-OH melatonin can quickly transition to its keto form i.e. 3-acetamidoethyl-5-methoxyindolin-2-one which is the most stable form[132] and has been detected consistently under experimental conditions.[133] The energy gap for the 3 reaction paths towards the formation of the different oxidation products are in the rage of (-0.1) - (-0.2) hartrees, i.e. an average of about -94 kcal/mol, with 2-OH melatonin path being the lowest as indicated in Table 5 and Figures 15-18.

Table 1: Enthalpy of reaction ΔH_r (in kcal/mol) for the oxidation of melatonin by hydroxyl radical at the Hartree-Fock level of theory

Molecule	HF/6-31G	HF/6-31G(d)	HF/cc-pVDZ	HF/cc-pVTZ	HF/cc-pVQZ
2-OH MLT	-56.4251975	-68.0445183	-72.74186	-73.25970	-78.44116
4-OH MLT	-52.9671975	-63.7348183	-68.37006	-70.3560	-74.18847
6-OH MLT	-46.8967975	-62.8420183	-62.68086	-64.28291	-65.86487

$$E_{total} = E_{elec} + \text{Zero point energy (ZPE)} \quad (2\text{-}115)$$

$$\Delta H_r = E_{total}(OH - MLT) + E_{total}(H_2O) - [E_{total}(MLT) + 2(E_{total}(OH)] \quad (2\text{-}116)$$

$$* E_{elec} = Eletronic\ energy$$

Table 2: Enthalpy of reaction (ΔH_r) (in kcal/mol) for the oxidation of melatonin by hydroxyl radical at the Density Functional Theory level of theory

Molecule	DFT/6-31G	DFT/6-31G(d)	DFT/cc-pVDZ	DFT/cc-pVTZ	DFT/cc-pVQZ
2-OH MLT	-103.38638	-105.95009	-109.84068	-117.17493	-115.16245
4-OH MLT	-98.35728	-106.46001	-102.67158	-97.78103	-104.81572
6-OH MLT	-91.25788	-106.112912	-108.48138	-110.00821	-112.00720

Table 3. Optimized geometry energies of melatonin and its oxidation products at the HF/cc-pVDZ, HF/cc-pVTZ , HF/cc-pVQZ and the HF CBS limits

Molecule	HF/cc-pVDZ	HF/cc-pVTZ	HF/cc-pVTZ	HF E_{CBS1}	HF E_{CBS2}
melatonin	-760.29707	-760.50210	-760.55119	-760.57426	-760.58621
2-OH MLT	-835.17469	-835.40262	-835.45667	-835.48283	-835.49478
4-OH MLT	-835.16754	-835.39626	-835.44990	-835.47675	-835.46633
6-OH MLT	-835.15758	-835.38688	-835.44130	-835.46407	-835.47968
OH radical	-75.39044	-75.41507	-75.421389	-75.42374	-765.42609
H_2O	-76.02739	-76.05832	-76.06658	-76.06922	-76.06958

*All energies are in hartrees (1 hartree= 2625.500kJ/mol, 1 hartree=627.5 kcal/mol)

Table 4. Optimized geometry energies of melatonin and its oxidation products at the DFT/B3LYP/cc-pVDZ, DFT/ B3LYP cc-pVTZ, DFT/ B3LYP /cc-pVQZ and the DFT/B3LYP/CBS limits

Molecule	DFT/cc-pvDZ	DFT/cc-pVTZ	DFT/cc-pVQZ	DFT E_{CBS3}	DFT E_{ECBS4}
Melatonin	-765.03532	-765.27315	-765.32706	-765.35684	-765.34286
2-OH MLT	-840.26482	-840.53589	-840.59529	-840.63123	-840.61196
4-OH MLT	-840.25318	-840.51663	-840.57775	-840.60973	-840.59621
6-OH MLT	-840.26251	-840.51498	-840.58923	-840.60372	-840.60912
OH radical	-75.73336	-75.76500	-75.77311	-75.77613	-75.77949
H_2O	-76.42185	-76.46126	-76.47075	-76.47513	-76.47377

*All energies are in hartrees (1 hartree= 2625.500kJ/mol, 1hartree=627.5 kcal/mol

Table 5: Enthalpy of reaction (ΔH_r) (in kcal/mol) for the oxidation of melatonin at HF and DFT CBS limit

Oxidation Product	HF/E_{CBS1}	HF/E_{CBS2}	DFT/E_{CBS3}	DFT/E_{CBS4}
2-OH MLT	-87.063413	-73.20549	-105.9655	-107.29300
4-OH MLT	-82.255298	-69.30479	-92.19234	-97.41940
6-OH MLT	-77.427124	-58.8449	-98.15868	-105.51166

$$\Delta H_{r(CBS)} = E_{total(CBS)}(OH - MLT) + E_{total(CBS)}(H_2O) - [E_{total(CBS)}(MLT) + 2(E_{total(CBS)}(OH)] \quad (2\text{-}117)$$

Table 6: Electronic energy gap values (ΔE) for the reaction of melatonin with hydroxyl radical at positions 2, 4, and 6 at HF and DFT CBS limit

Oxidation Product	HF/ΔE_{CBS1}	HF/ΔE_{CBS2}	DFT/ΔE_{CBS3}	DFT/ΔE_{CBS4}
2-OH MLT	-0.13189	-0.12835	-0.19732	-0.18390
4-OH MLT	-0.12422	-0.12214	-0.17537	-0.16816
6-OH MLT	-0.11653	-0.10547	-0.18488	-0.18106

$$\Delta E = E_{elec}(OH - MLT\ ) + E_{elec}(H_2O) - [E_{elec}(MLT) + 2(E_{elec}(OH)] \quad (2\text{-}118)$$

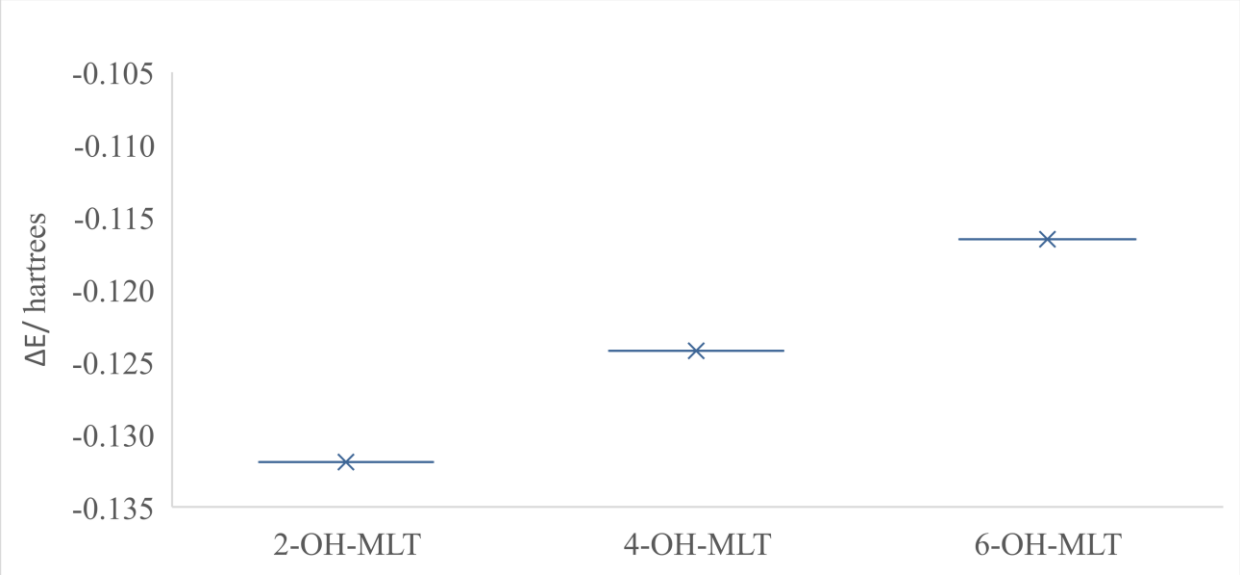

Figure 15: Electronic energy gap chart of the oxidation products of melatonin at the HF CBS limit calculated from E_{CBS1}

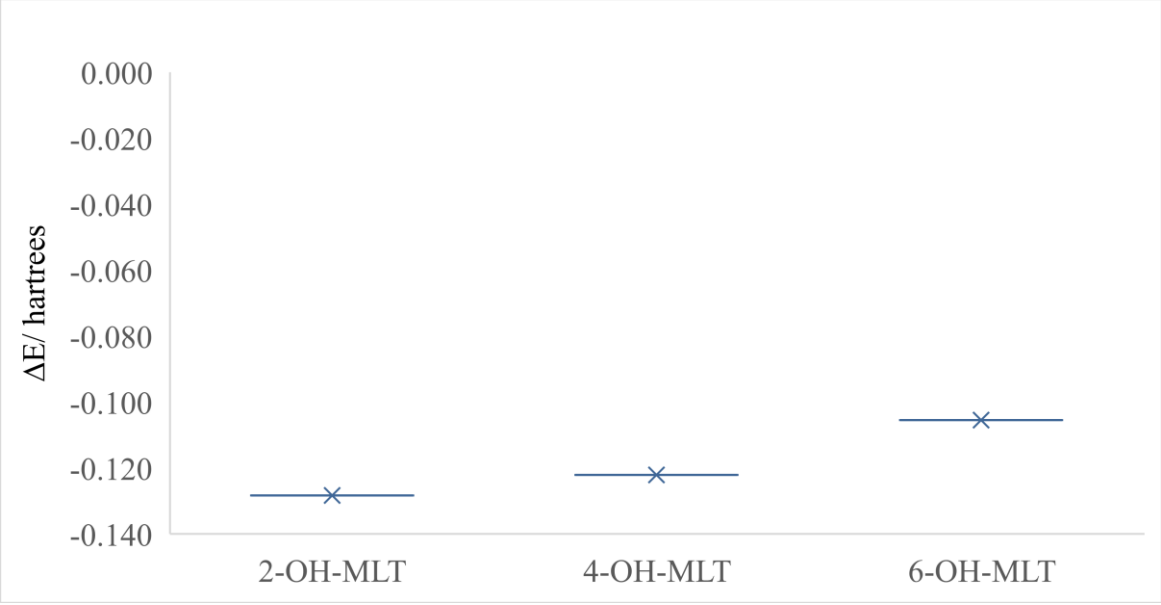

Figure 16: Electronic energy gap chart of the oxidation products of melatonin at the HF CBS limit calculated from E_{CBS2}

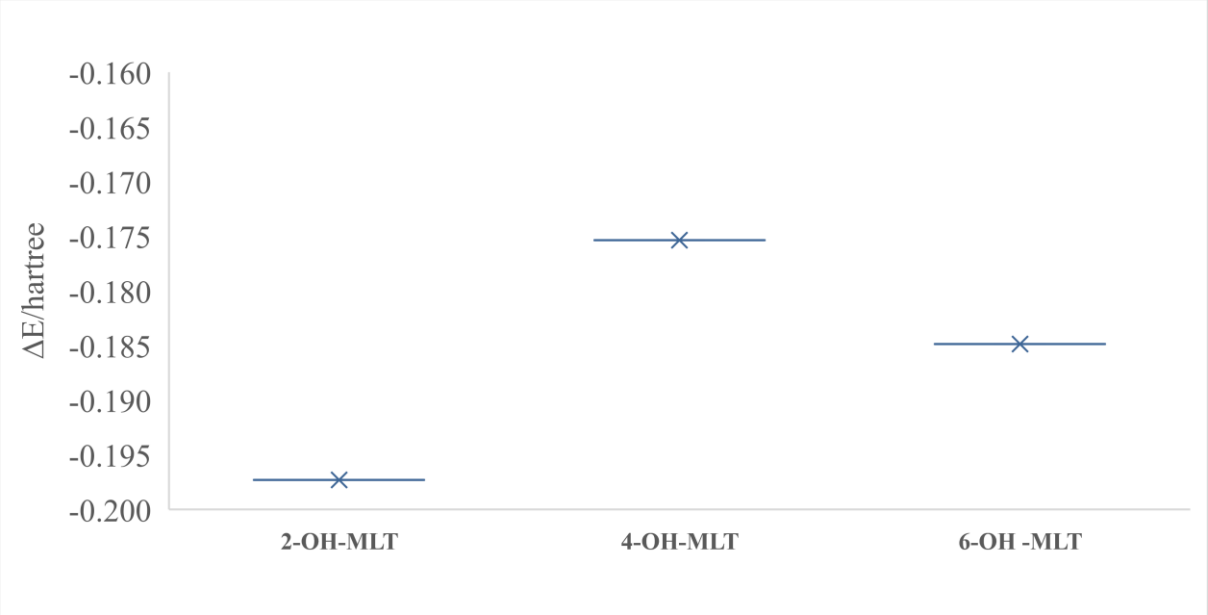

Figure 17: Electronic energy gap chart of the oxidation products of melatonin at the HF CBS limit calculated from E_{CBS3}

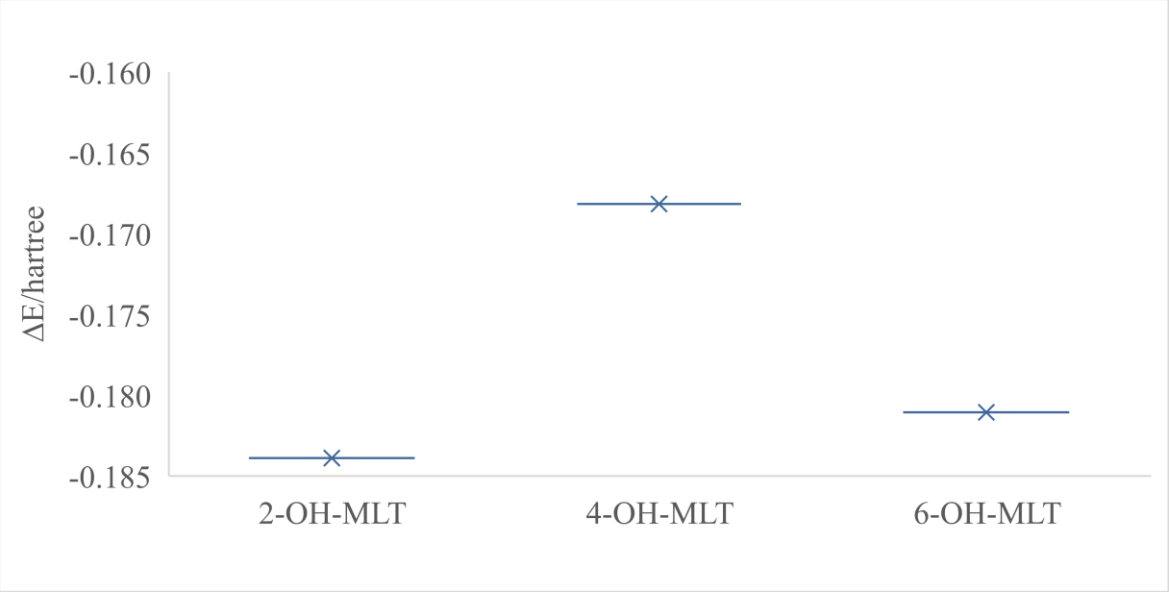

Figure 18: Electronic energy gap chart of the oxidation products of melatonin at the HF CBS limit calculated from E_{CBS4}

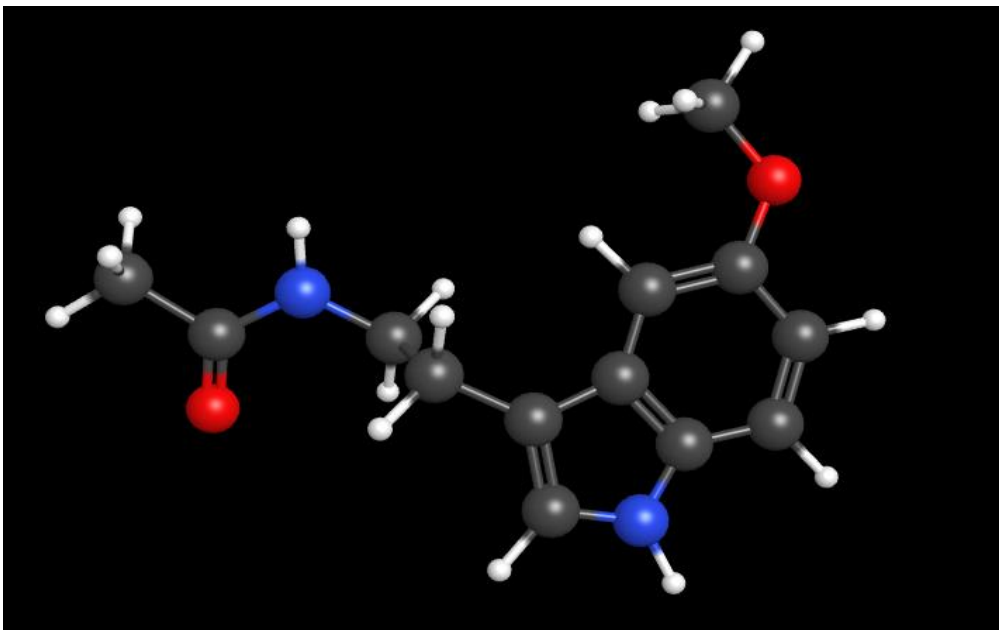

Figure 19: Structure of optimized geometry of melatonin

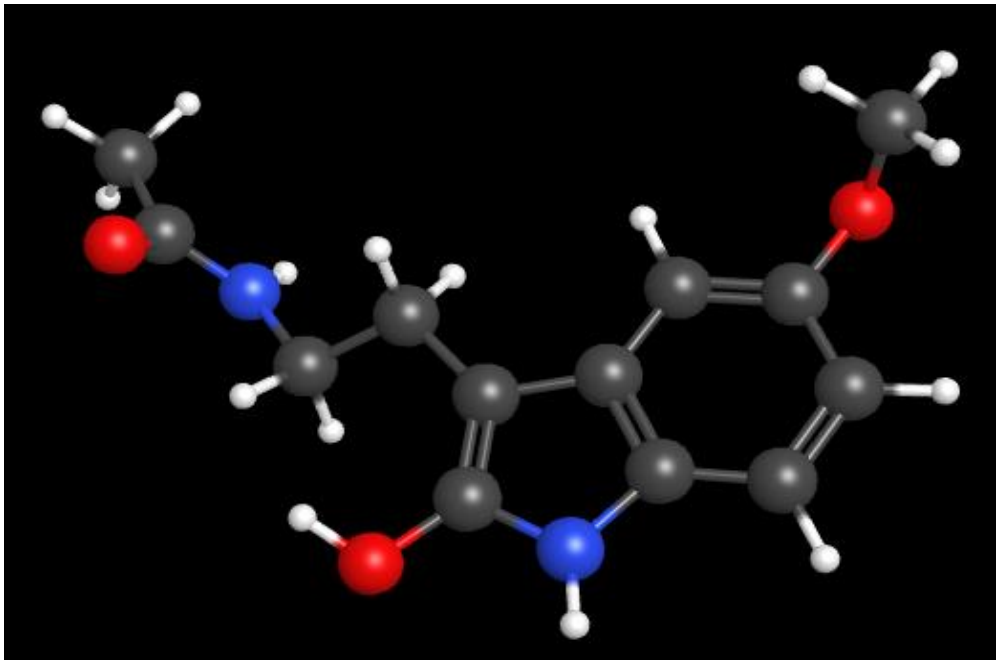

Figure 20: Structure of optimized geometry of 2-OH-MLT

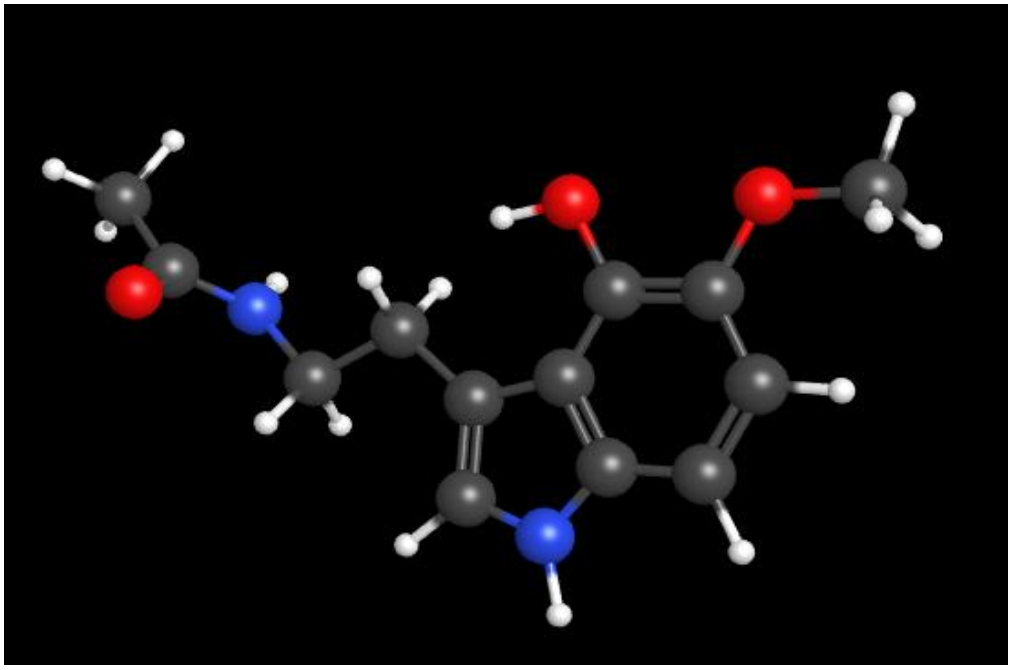

Figure 21: Structure of optimized geometry of 4-OH-MLT

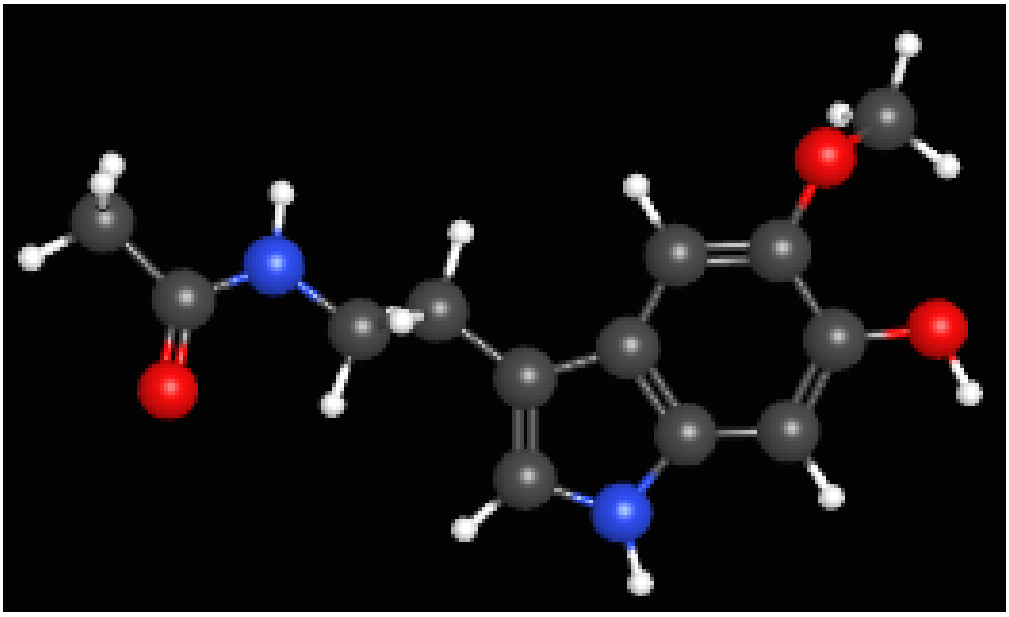

Figure 22: Structure of optimized geometry of 6-OH-MLT

However, there is no clear distinction between 4-OH-MLT and 6-OH-MLT as the energy gap as indicated in Figures 15-18 is not consistent between different levels of theory used herein. The stability of 2-OH-MLT indicates that the radical intermediates formed via the 2-OH melatonin path will be more stable and may support the hypothesis of melatonin as a spin trap since the stable compound has a longer lifetime as compared to isolated hydroxyl radical. However, the 2-OH melatonin may not be used as a further spin trap because of its increased stability of the keto form making it unreactive towards free radicals. 4-OH and 6-OH melatonin, on the other hand, may still function as spin traps since they do not form any stable tautomer.

Conclusion

The mechanism of reaction indicated in Figures 11-13 shows a multi-step reaction during the oxidation of melatonin by hydroxyl radical and proceed via addition of radical to the indole ring to generate a neutral indolyl radical. This type of reaction is known to be exothermic according to previous works[79] and our research clearly support this fact as all the reactions are exothermic.

The electronic energies obtained from the optimized geometry shows large drop in energies of the oxidation products compared to the parent melatonin. The energy gap for all products is between (-0.1) – (-0.2) hartrees and an average of about -94kcal/mol. Calculation of the enthalpy of reactions indicates that all the three reaction paths are exothermic. The enthalpy of reaction of the of 2-OH-MLT path appears to much lower indicating a more stable intermediate. This observation is quite reasonable because 2-OH-MLT is in equilibrium with its keto form i.e. 3-acetamidoethyl-5-methoxyindolin-2-one and this keto form is more stable.

Also, the heat of reaction is lower for 2-OH-MLT as compared to both 4-OH-MLT and 6-OH-MLT. The low energy of the oxidation products compared to the parent melatonin indicate a stable radical intermediate, with 2-OH-MLT having the lowest energy. This would lengthen the lifetime of the radical intermediate and thus enable easier characterization with ESR spectroscopy. Therefore, this work supports the possibility of using melatonin as a spin trap, but further investigation is necessary.

CHAPTER 4. FUTURE WORK

In the future, it will be necessary to include the kinetics of the reaction of melatonin with hydroxyl radical. Therefore, the energy of transition states thus the activation energy should be calculated, and many kinetics data can be evaluated. All of the reactions in this work are in gas phase thus, an aqueous medium (with varying pH) calculation might be necessary to better mimic the biological medium. Consequently, extensive theoretical calculations should establish why 2-OH melatonin is far more stable than any of the oxidation products of melatonin. A semi-empirical calculation should be performed alongside the *ab initio* calculations to further elucidate the reaction mechanism. For some nitrones such as DMPO, the spin adduct of hydroxyl and superoxide are not easily distinguished because DMPO-superoxide adduct can spontaneously decay in to DMPO-hydroxyl adduct.[134] Therefore, future work should calculate the theoretical EPR spectra of the melatonin-hydroxyl-adduct, melatonin derivatives-hydroxyl adduct, and other various spin radical adducts to determine if the spectra are distinguishable. This will enable evaluation of the spin trapping ability of melatonin. Furthermore, the calculation should be extended to the augmented Dunning's basis set, aug-cc-pVXZ, (X=D, T, Q).

REFERENCES

(1) Droge, W.; Droge, W. Free Radicals in the Physiological Control of Cell Function. *Physiol Rev.* **2002**, 82, 47–95.

(2) Lobo, V.; Patil, A.; Phatak, A.; Chandra, N. Free Radicals, Antioxidants and Functional Foods: Impact on Human Health. *Pharmacogn. Rev.* **2010,** 4, 118.

(3) Cheeseman, K. H.; Slater, T. F. An Introduction to Free Radicals. *Choice Rev. Online* **2013,** 31, 31-2692-31–2692.

(4) Kabel, A. Free Radicals and Antioxidants: Role of Enzymes and Nutrition. *World J. Nutr. Heal*. **2014,** 2, 35–38.

(5) Lin, M. T.; Beal, M. F. Mitochondrial Dysfunction and Oxidative Stress in Neurodegenerative Diseases. *Nature* **2006,** 443, 787–795.

(6) Kanski, J.; Aksenova, M.; Stoyanova, A.; Butterfield, D. A. Ferulic Acid Antioxidant Protection against Hydroxyl and Peroxyl Radical Oxidation in Synaptosomal and Neuronal Cell Culture Systems in Vitro: Structure-Activity Studies. *J. Nutr. Biochem*. **2002,** 13, 273–281.

(7) Ieter; Moncol, J.; Cronin, M. T. D.; Mazur, M.; Telser, JoshuaValko, M.; Leibfritz, D. Free Radicals and Antioxidants in Normal Physiological Functions and Human Disease. *Int. J. Biochem. Cell Biol.* **2007,** 39, 44–84.

(8) Katoch, N.; Kaur, P.; Kashyap, P.; Gupta, S.; Dahiya, R. S. Role of Oxidative Stress in Cardiovascular Diseases. *Res. J. Pharm. Biol. Chem. Sci*. **2013,** 4, 870–881.

(9) Barry D; Christiaan L. Aging and the Role of Reactive. *Ann. N.Y. Acad. Sci.* **2002**, 959, 66-81

(10) Shin, I. S.; Shin, N. R.; Park, J. W.; Jeon, C. M.; Hong, J. M.; Kwon, O. K.; Kim, J. S.; Lee, I. C.; Kim, J. C.; Oh, S. R.; et al. Melatonin Attenuates Neutrophil Inflammation and Mucus Secretion in Cigarette Smoke-Induced Chronic Obstructive Pulmonary Diseases via the Suppression of Erk-Sp1. *Signaling. J. Pineal Res.* **2015,** 58, 50–60.

(11) Finkel, T. Radical Medicine: Treating Ageing to Cure Disease. *Nat. Rev. Mol. Cell Biol.* **2005,** 6, 971–976.

(12) Chiarugi, P.; Fiaschi, T. Redox Signalling in Anchorage-Dependent Cell Growth. *Cell Signal.* **2007,** 19, 672–682.

(13) Murphy, M. P. How Mitochondria Produce Reactive Oxygen Species. *Biochem. J.* **2009,** 417, 1–13.

(14) Kim, G. H.; Kim, J. E.; Rhie, S. J.; Yoon, S. The Role of Oxidative Stress in Neurodegenerative Diseases. *Exp. Neurobiol.* **2015,** 24, 325-340.

(15) Zeeshan, H. M. A.; Lee, G. H.; Kim, H. R.; Chae, H. J. Endoplasmic Reticulum Stress and Associated ROS. *Int. J. Mol. Sci*. **2016,** 17, 1–20.

(16) Bagchi K.; Puri S. Free radicals and antioxidants in health and disease. *La Revenue Santè de la Mèditerranèe Orientale.* **1998,** 4, 350-360.

(17) Deby, C.; Goutier, R. New Perspectives on the Biochemistry of Superoxide Anion and the Efficiency of Superoxide Dismutases. *Biochem. Pharmacol.* **1990,** 39, 399–405.

(18) Infanger, D. W.; Sharma, R. V.; Davisson, R. L. NADPH Oxidases of the Brain: Distribution, Regulation, and Function. *Antioxid. Redox Signal.* **2006,** 8, 1583–1596.

(19) Palmer, R. M. J.; Rees, D. D.; Ashton, D. S.; Moncada, S. L-Arginine Is the Physiological Precursor for the Formation of Nitric Oxide in Endothelium-Dependent Relaxation. *Biochem. Biophys. Res. Commun.* **1988,** 153, 1251–1256.

(20) Velkov, Z. A.; Velkov, Y. Z.; Galunska, B. T.; Paskalev, D. N.; Tadjer, A. V. Melatonin: Quantum-Chemical and Biochemical Investigation of Antioxidant Activity. *Eur. J. Med. Chem.* **2009,** 44, 2834–2839.

(21) Haber, F. The Catalytic Decomposition of Hydrogen Peroxide by Iron Salts. *Proc. - R. Soc. Phys. Eng. Sci.* **1934,** 147, 332.

(22) Fenton, H. Oxidation of Tartaric Acid in the presence of iron. *J. Chem. Soc. Trans.* **1894**, 65, 899-910

(23) Barb W.G.; George, P.; Hargrave, K. R. Reaction of Ferrous and Ferric Ions with Hydrogen Peroxide. *Trans. Faraday Soc*. **1950,** 47, 591–616.

(24) Walling, C. Fenton's Reagent Revisited. *Acc. Chem. Res.* **1975,** 8, 125-131

(25) Crichton, R. R.; Charloteaux-wauters, M. Iron Transport and Storage. *Nature.* **1976,** 260, 466–466.

(26) Stone, D.; Whalley, L. K.; Heard, D. E. Tropospheric OH and HO2 radicals: Field Measurements and Model Comparisons. *Chem. Soc. Rev.* **2012,** 41, 6348–6404.

(27) Ross, F.; Ross, B. NSRDS Selected Specific Rates of Reactions of Transients from Water in Aqueous Solution. III. Hydroxyl Radical and Perhydroxyl Radical and Their Radical Ions; *Nat. Stand. Ref. Data Ser.Nat. Bur. Stand. (U.S.),***1977**, 59, 1-122.

(28) Pan, X.; Bastian, E.; Von Sonntag, C. The reactions of hydroxyl radicals with 1,4- and 1,3-cyclohexadiene in aqueous solution: A pulse radiolysis and product study radiolysis, **1988**, 43, 1201-1205.

(29) Atkinson, R.; Aschmann, S. M.; Arey, J. Formation of Ring Retaining Products from the OH Radical-initated Reactions of O-, M-, and P-xylene. *Int. J. Chem. Kinet.* **1991,** 23, 77–97.

(30) Greenberg, M. M. Pyrimidine Nucleobase Radical Reactivity in DNA and RNA. *Radiat. Phys. Chem.* **2016,** 128, 82–91.

(31) Janzen, E. G. Spin Trapping. *Acc. Chem. Res.* **1971**, *4*, 31–40.

(32) Evans, C. A. Spin Trapping. *Aldrichimica Acta* **1979,** 12, 23–29.

(33) Pou, S.; Halpern, H. J.; Tsai, P.; Rosen, G. M. Issues Pertinent to the in Vivo in Situ Spin Trapping of Free Radicals. *Acc. Chem. Res.* **1999,** 32, 155–161.

(34) Jeremić, S.; Amić, A.; Stanojević-Pirković, M.; Marković, Z. Selected Anthraquinones as Potential Free Radical Scavengers and P-Glycoprotein Inhibitors. *Org. Biomol. Chem.* **2018,** 16, 1890–1902.

(34) Sawant, P. Potential Use of Spin Traps to Control ROS in Antipollution Cosmetics—A Review. *Cosmetics* **2018,** 5, 1-14.

(35) Makarova, K.; Łastawska, K.; Wagner, D.; Wawer, I. ESR study of spin trapping in Fenton media in the presence of taxifolin. *J. Mol. Struct.* **2014,** 1067, 27-36.

(36) Nakarada, Đ.; Petković, M. Mechanistic Insights on How Hydroquinone Disarms OH and OOH Radicals. *Int. J. Quantum Chem*. **2018,** 118, 1–14.

(37) Khan, N.; Wilmot, C. M.; Rosen, G. M.; Demidenko, E.; Sun, J.; Joseph, J.; O'Hara, J.; Kalyanaraman, B.; Swartz, H. M. Spin Traps: In Vitro Toxicity and Stability of Radical Adducts. *Free Radic. Biol. Med.* **2003**, *34*, 1473–1481

(38) Cerón-Carrasco, J. P.; Roy, H. M.; Cerezo, J.; Jacquemin, D.; Laurent, A. D. Theoretical Insights on the Antioxidant Activity of Edaravone Free Radical Scavengers Derivatives. *Chem. Phys. Lett.* **2014,** 599, 73–79.

(39) Barclay, L. R. C.; Vinqvist, M. R. Do Spin Traps Also Act as Classical Chain-Breaking Antioxidants? A Quantitative Kinetic Study of Phenyl Tert-Butylnitrone (PBN) in Solution and in Liposomes. *Free Radic. Biol. Med.* **2000,** 28, 1079–1090.

(40) Rehorek, D.; Hennig, H.; Dubose, C. M.; Kemp, T. J.; Janzen, E. G. Spin Trapping of Inorganic Radicals. *Free Radic. Res.* **1990,** 10, 75–84.

(41) Dikalova, A. E.; Kadiiska, M. B.; Mason, R. P. An in Vivo ESR Spin-Trapping Study: Free Radical Generation in Rats from Formate Intoxication - Role of the Fenton Reaction. *Proc. Natl. Acad. Sci. U. S. A.* **2001,** 98, 13549–13553.

(42) Yashige K. Pharmacologic Properties of Phenyl N-tert-Butylnitrone. *J. Chem. Inf. Model.* **2019,** 53, 1689-1699.

(43) Floyd, R. A.; Hensley, K.; Forster, M. J.; Kelleher-Andersson, J. A.; Wood, P. L. Nitrones, Their Value as Therapeutics and Probes to Understand Aging. *Mech. Ageing Dev*. **2002,** 123, 1021–1031.

(44) Reiter R. J.; Tan, D.; Osuna, C.; Gitto. Action of melatonin in the Reduction of Oxidative *Stress. J. Biomed Sci.* **2000,** 3900, 444–458

(45) Buettner, G. R.; Mason, R. P. Spin-Trapping Methods for Detecting Superoxide and Hydroxyl Free Radicals in Vitro and in Vivo. *Methods Enzymol.* **1990**, *186*, 127–133

(46) Berliner, L., 2003. Spin Trapping in Vivo: Facts and Artifacts. In: Timmins G. and Liu, K. ed., *In Vivo EPR (ESR): Theory and Application*, 10th ed. Boston: Springer, US, pp.285-308.

(47) Reiter, R. J. Pineal Melatonin: Cell Biology of Its Synthesis and of Its Physiological Interactions. *Endocr. Rev.* **1991,** 12, 151–180.

(48) Reiter, R. J. Melatonin: The Chemical Expression of Darkness. *Mol. Cell. Endocrinol.* **1991,** 79, 1–3.

(49) Lerner, A.; Case, J.; Takahashi, Y.; Lee, T.; Mori, W. Isolation of Melatonin, the Pineal Gland Hormone Factor the Lightens Melanocytes. *J. Am. Chem. Soc.* **1958,** 80, 10, 2587-2587.

(50) Lerner, A. B.; Case, J. D.; Heinzelman, R. V. Structure of Melatonin. *J. Am. Chem. Soc.* **1959,** 81 (22), 6084–6085.

(51) Bergego, C.; Pelleg-Toiba, R.; Wollberg, Z. Effect of pyridoxine deficiency on aromatic L-amino acid decarboxylase in adult rat brain. *Exp. Brain Res.* **1981,** 337–350.

(52) Coon, S. L.; Roseboom, P. H.; Baler, R.; Weller, J. L.; Namboodiri, M. A. A.; Koonin, E. V.; Klein, D. C. Pineal Serotonin N-Acetyltransferase: Expression Cloning and Molecular Analysis. *Science*. **1995,** 270, 1681–1683.

(53) Axelrod J.; Weissbach H. Enzymatic O-Methylation of N-Acetylserotonin to Melatonin *Science* **1960,** 131, 1312.

(54) Tosini, G.; Menaker, M. The Clock in the Mouse Retina: Melatonin Synthesis and Photoreceptor Degeneration. Brain Res. **1998,** 789, 221–228.

(55) Liu, C.; Fukuhara, C.; Wessel, J. H.; Iuvone, P. M.; Tosini, G. Localization of Aa-Nat MRNA in the Rat Retina by Flourescence in Situ Hybridization and Laser Capture Microdissection. *Cell Tissue Res.* **2004,** 315, 197–201.

(56) Sobolevskaya, I. S.; Zykova, O. S.; Myadelets, O. D. The Role of Melatonin in the Physiology and Pathology of the Skin. Klin. *Endocrine.* **2019,** 27, 137-147.

(57) Champier, J.; Claustrat, B.; Besancon, R.; Eymin, C.; Killer, C.; Jouvet, A.; Chamba, G.;, Fèvre-Montage M. Evidence For Tryptophan Hydroxylase And Hydroxy-Indol-O-Methyl- Transferase mRNAs in Human Blood Platelets,. 1997, 60, 2191–2197.

(58) Carrillo-Vico, A.; Calvo, J. R.; Abreu, P.; Lardone, P. J.; García-Mauriño, S.; Reiter, R. J.; Guerrero, J. M. Evidence of Melatonin Synthesis by Human Lymphocytes and Its Physiological Significance: Possible Role as Intracrine, Autocrine, and/or Paracrine Substance. *FASEB J.* 2004, 18, 537–539.

(59) Bubenik, G. A. Gastrointestinal Melatonin: Localization, Function, and Clinical Relevance. *Dig. Dis. Sci.* **2002,** 47, 2336–2348.

(60) Conti, A.; Conconi, S.; Hertens, E.; Skwarlo-Sonta, K.; Markowska, M.; Maestroni, G. J. M. Evidence for Melatonin Synthesis in Mouse and Human Bone Marrow Cells. *J. Pineal Res.* **2000,** 28, 193–202.

(61) Tan, D. X.; Manchester, L. C.; Reiter, R. J.; Qi, W. B.; Zhang, M.; Weintraub, S. T.; Cabrera, J.; Sainz, R. M.; Mayo, J. C. Identification of Highly Elevated Levels of Melatonin in Bone Marrow: Its Origin and Significance. Biochem. Biophys. *Acta - Gen. Subj.* **1999,** 1472, 206–214.

(62) Tan, D.; Manchester, L. C.; Reiter, R.; Qi, W.; Hanes, M. a; Farley, N. J. Reiter*, Wenbo Qi, 1 Martha A. Hanes. High Physiological Levels of Melatonin in the Bile of Mammals. *Life Sciences.* **1999**, 65, 2523–2529.

(63) Skinner, D. C.; Malpaux, B. High Melatonin Concentrations in Third Ventricular Cerebrospinal Fluid Are Not Due to Galen Vein Blood Recirculating Through the Choroid Plexus. Endocrinology **1999,** 140, 4399–4405.

(64) Dubocovich, M. L.; Markowska, M. Functional MT 1 and MT 2 Melatonin Receptors in Mammals. *Endocrine.* **2005,** 27, 101–110.

(65) Pandi-Perumal, S. R.; Trakht, I.; Srinivasan, V.; Spence, D. W.; Maestroni, G. J. M.; Zisapel, N.; Cardinali, D. P. Physiological Effects of Melatonin: Role of Melatonin Receptors and Signal Transduction Pathways. *Prog. Neurobiol.* **2008,** 85, 335–353.

(66) Arendt, J. Melatonin and Human Rhythms. Chronobiol. Int. **2006,** 23, 21–37.

(67) Lewy, A.; Emens, J.; Jackman, A.; Yuhas, K. Circadian Uses of Melatonin in Humans. *Chronobiol. Int.* **2006,** 23, 403–412.

(68) Reiter, R. J.; Tan, D.-X.; Manchester, L. C.; Paredes, S. D.; Mayo, J. C.; Sainz, R. M. Melatonin and Reproduction Revisited. *Biol. Reprod.* **2009,** 81, 445–456.

(69) Carrillo-Vico, A.; Lardone, P. J.; Álvarez-Śnchez, N.; Rodrĩguez-Rodrĩguez, A.; Guerrero, J. M. Melatonin: Buffering the Immune System. *Int. J. Mol. Sci.* **2013,** 14, 8638–8683.

(70) Hardeland, R. Melatonin and 5-Methoxytryptamine in Non-Metazoans. *Reprod. Nutr. Dev.* **1999,** 39, 399–408.

(71) Fuhrberg, B.; Balzer, I.; Hardeland, R.; Werner, A.; Lüning, K. The Vertebrate Pineal Hormone Melatonin Is Produced by the Brown Alga Pterygophora Californica and Mimics Dark Effects on Growth Rate in the Light. *Planta.* **1996,** 200, 125–131.

(72) Lu, D.; Song, L.; Li, F. Uniform Asymptotics for Discounted Aggregate Claims in Dependent Multi-Risk Model. *Commun. Stat. - Theory Methods.* **2018,** 269, 1–13.

(73) Ianas, O.; Olinescu, R.; Bădescu, I. Melatonin involvement in oxidative processes. *Endocrinologie.* **1991.** 29. 147-53.

(74) Hardeland, R.; Reiter, R. J.; Poeggeler, B.; Tan, D. X. The Significance of the Metabolism of the Neurohormone Melatonin: Antioxidative Protection and Formation of Bioactive Substances. *Neurosci. Biobehav. Rev.* **1993,** 17, 347–357.

(75) Jahnke, G.; Marr, M.; Myers, C.; Wilson, R.; Travlos, G.; Price, C. Maternal and Developmental Toxicity Evaluation of Melatonin Administered Orally to Pregnant Sprague-Dawley Rats. *Toxicol. Sci.* **1999,** 50, 271–279.

(76) Ceraulo, L.; Ferrugia, M.; Tesoriere, L.; Segreto, S.; Livrea, M. A.; Turco Liveri, V. Interactions of Melatonin with Membrane Models: Portioning of Melatonin in AOT and Lecithin Reversed Micelles. *J. Pineal Res.* **1999,** 26, 108–112.

(77) Bonnefont-Rousselot, D.; Collin, F. Melatonin: Action as Antioxidant and Potential Applications in Human Disease and Aging. *Toxicology* **2010,** 278, 55–67.

(78) Galano, A.; Tan, D. X.; Reiter, R. J. On the Free Radical Scavenging Activities of Melatonin's Metabolites, AFMK and AMK. *J. Pineal Res.* **2013,** 54, 245–257.

(79) Turjanski, A. G.; Rosenstein, R. E.; Estrin, D. A. Reactions of Melatonin and Related Indoles with Free Radicals: A Computational Study. *J. Med. Chem.* **1998,** 41, 3684–3689.

(80) Kładna, A.; Aboul-Enein, H. Y.; Kruk, I. Enhancing Effect of Melatonin on Chemiluminescence Accompanying Decomposition of Hydrogen Peroxide in the Presence of Copper. *Free Radic. Biol. Med.* **2003,** 34, 1544–1554.

(81) Collin, F.; Bonnefont-Rousselot, D.; Yous, S.; Marchetti, C.; Jore, D.; Gardès-Albert, M. Online H/D Exchange Liquid Chromatography as a Support for the Mass Spectrometric Identification of the Oxidation Products of Melatonin. *J. Mass Spectrom.* **2009,** 44, 318–329

(82) Itoh, M. T.; Ishizuka, B.; Kudo, Y.; Fusama, S.; Amemiya, A.; Sumi, Y. Detection of Melatonin and Serotonin N-Acetyltransferase and Hydroxyindole-O-Methyltransferase Activities in Rat Ovary. *Mol. Cell. Endocrinol.* **1998**, 136, 7–13.

(83) Ressmeyer, A. R.; Mayo, J. C.; Zelosko, V.; Sáinz, R. M.; Tan, D. X.; Poeggeler, B.; Antolín, I.; Zsizsik, B. K.; Reiter, R. J.; Hardeland, R. Antioxidant Properties of the Melatonin Metabolite N1-Acetyl-5-Methoxykynuramine (AMK): Scavenging of Free Radicals and Prevention of Protein Destruction. *Redox Rep.* **2003,** 8, 205–213.

(84) Álvarez-Diduk, R.; Galano, A.; Tan, D. X.; Reiter, R. J. N-Acetylserotonin and 6-Hydroxymelatonin against Oxidative Stress: Implications for the Overall Protection Exerted by Melatonin. *J. Phys. Chem. B* **2015,** 119, 8535–8543.

(85) Longoni, B.; Pryor, W. A.; Marchiafava, P. Inhibition of Lipid Peroxidation by N-Acetylserotonin and Its Role in Retinal Physiology. *Biochem. Biophys. Res. Commun.* **1997,** 233, 778–780.

(86) García, J. J.; Reiter, R. J.; Karbownik, M.; Calvo, J. R.; Ortiz, G. G.; Tan, D. X.; Martínez-Ballarín, E.; Acua-Castroviejo, D. N-Acetylserotonin Suppresses Hepatic Microsomal Membrane Rigidity Associated with Lipid Peroxidation. *Eur. J. Pharmacol.* **2001,** 428, 169–175.

(87) Zavodnik, I. B.; Domanski, A. V.; Lapshina, E. A.; Bryszewska, M.; Reiter, R. J. Melatonin Directly Scavenges Free Radicals Generated in Red Blood Cells and a Cell-Free System: Chemiluminescence Measurements and Theoretical Calculations. *Life Sci.* **2006,** 79, 391–400.

(88) Reiter, R. J.; Tan, D.; Terron, M. P.; Flores, L. J.; Czarnocki, Z. Melatonin and Its Metabolites: New Findings Regarding Their Production and Their Radical Scavenging Actions. *Acta Biochim. Pol.* **2007,** 54, 1–9.

(89) Galano, A.; Castañeda-Arriaga, R.; Pérez-González, A.; Tan, D. X.; Reiter, R. J. Phenolic Melatonin-Related Compounds: Their Role as Chemical Protectors against Oxidative Stress. *Molecules* **2016,** 21, 1-42.

(90) Maharaj, D. S.; Maharaj, H.; Antunes, E. M.; Maree, D. M.; Nyokong, T.; Glass, B. D.; Daya, S. 6-Hydroxymelatonin Protects against Quinolinic-Acid-Induced Oxidative Neurotoxicity in the Rat Hippocampus. *J. Pharm. Pharmacol.* **2005,** 57, 877–881.

(91) Allegra, M.; Reiter, R. J.; Tan, D. X.; Gentile, C.; Tesoriere, L.; Livrea, M. A. The Chemistry of Melatonin's Interaction with Reactive Species. *J. Pineal Res.* **2003**, *34*, 1–10.

(92) Galano, A.; Tan, D. X.; Reiter, R. J. Cyclic 3-Hydroxymelatonin, a Key Metabolite Enhancing the Peroxyl Radical Scavenging Activity of Melatonin. *RSC Adv.* **2014**, *4*, 5220–5227.

(93) Pryor, W. A. Free Radicals in Organic Chemistry. *Free Radic. Biol. Med.* **1996**, *21* (2), 253–254.

(94) Miglicava E.; Ancerewicz, J.; Carrupt P.; Testa, B. Theoretical Parameters to Characterize Antioxidants, Part 2; The cases of Melatonin and Carvedilol. *Helv. Chim. Acta.* **1998,** 81, 1337–1348.

(95) Galano, A. A First Principles Investigation on the Electron Donor Ability of Synthetic Melatonin Derivatives: Implications for Their Antioxidant Activity. *Theor. Chem. Acc.* **2016,** 135, 28–33.

(96) Schrodinger, E. Quantisierung Als Eigmwertproblem. *Ann. Phys.* **1926,** 13, 438–490.

(97) Schrodinger, E. Quantisierung Als Eigenwertproblem - Dritte Mitteilung. *Ann. Phys.***1926,** 385, 437–490.

(98) Schrödinger, E. Quantisierung Als Eigenwertproblem IV. *Ann. Phys.* **1926,** 386, 109-139.

(99) Born, M. Zur Quantenmechanik Der Stoßvorgänge. Zeitschrift für *Phys.* **1926,** 37, 863–867.

(100) Levine, I. N., Quantum Chemistry. 7th ed.; Pearson: Boston, **2014.**

(101) Heisenberg, W. Über Den Anschaulichen Inhalt Der Quantentheoretischen Kinematik Und Mechanik. Zeitschrift für *Phys.* **1927,** 43, 172–198.

(102) Terme, D.; Beitrag, S.; Grund, D.; Standpunkte, V. *Der Physik* 1. **1927,** 20, 457-484

(103) Hartree, D. The Wave Mechanics of an Atom with a Non-Coulomb Central Field. Part I. Theory and Methods. *Math. Proc. Cambridge Philos. Soc.* **1928,** 24, 89–110.

(104) Slater, J. C., Atomic Shielding Constants. *Phys. Rev.* **1930,** 36, 57-64.

(105) Fock, V. Näherungsmethode Zur Lösung Des Quantenmechanischen Mehrkörperproblems. Zeitschrift für *Phys*. **1930,** 61, 126–148.

(106) Roothaan, C. C. J., New Developments in Molecular Orbital Theory. *Rev. Mod. Phys.* **1951,** 23, 69-89.

(107) Roothaan, C. C. J. Self-Consistent Field Theory for Open Shells of Electronic Systems. *Rev. Mod. Phys.* **1960,** 32, 179185.

(108) Hohenberg P.; Kohn W. Inhomogeneous Electron Gas. *Phys. Rev*., **1964**, 136**,** B864-B871.

(109) Kohn W.; Sham L. J. Self-Consistent Equations Including Exchange and Correlation Effects *Phy. Rev.* **2002,** 41, 892–893.

(110) Becke A.D. Density-functional Exchange-Energy Approximation with Correct Asymptotic Behavior. *J. Chem. Phys.* **1988,** 4, 276–282.

(111) Becke, A. D. Density-Functional Thermochemistry. III. The Role of Exact Exchange. *J. Chem. Phys*. **1993,** 98, 5648–5652.

(112) Chengteh, L.; Weitao, Y.; Robert, G. Development of the Colle-Salvetti corelation-energy formula into a functional of the electron density. *Phys. rev. B.* **1988** 37(2) 785-789.

(113) Stephens, P. J.; Delvin, F. J.; Chabalowski, C.F.; Frisch M. JAb Initio Calculation of Vibrational Absorption and Circular Dichroism Spectra Using Density Functional Force Fields. *J. Chem.,* **1994,** 98, 11623-11627.

(114) Vosko, S. H.; Wilk, L.; Nusair, M. Accurate Spin-Dependent Electron Liquid Correlation Energies for Local Spin Density Calculations: A Critical Analysis. Can. *J. Phys.* **1980,** 58, 1200–1211.

(115) Boys, S. F. Electronic Wave Functions. I. A General Method of Calculation for the Stationary States of Any Molecular System. *Proc. R. Soc. Lond. A* **1950**, 200, 542-554

(116) Pople, J. A. Quantum Chemical Models (Nobel Lecture). *Angew. Chemie Int. Ed*. **1999,** 38, 1894–1902.

(117) Dunning T.H., Hay P.J. (1977) Gaussian Basis Sets for Molecular Calculations. In: Schaefer H.F. (eds) Methods of Electronic Structure Theory. Modern Theoretical Chemistry, vol 3. Springer, Boston, MA, **1977**; pp 20-27.

(118) Dunning, T. H. Gaussian Basis Sets for Use in Correlated Molecular Calculations. I. The Atoms Boron through Neon and Hydrogen. *J. Chem. Phys.* **1989,** 1007–1023.

(119) Kendall, R. A.; Dunning, T. H., Jr.; Harrison, R. J., Electron affinities of the first-row atoms revisited. Systematic basis sets and wave functions. *J. Chem. Phys.* **1992,** 96, 6796-6806.

(120) Woon, D. E.; Dunning, T. H. Gaussian Basis Sets for Use in Correlated Molecular Calculations. III. The Atoms Aluminum through Argon. *J. Chem. Phys.* **1993,** 98, 1358–1371.

(121) Peterson, K. A.; Woon, D. E.; Dunning, T. H.; Peterson, K. A.; Woon, D. E.; Dunning, T. H. Benchmark Calculations with Correlated Molecular Wave Functions. IV. The Classical Barrier Height of the H + H2 → H2 + H Reaction Benchmark Calculations with Correlated Molecular Wave Functions. **1994,** 100, 7410-7415.

(122) Wilson, A. K.; van Mourik, T.; Dunning, T. H., Gaussian basis sets for use in correlated molecular calculations. VI. Sextuple zeta correlation consistent basis sets for boron through neon. *Theochem,* **1996** 388, 339-349.

(123) Martin, J.L. Ab Initio Total Atomization Energies of Small Molecules - towards the Basis Set Limit. *Chem. Phys. Lett.* **1996,** 259, 669-678.

(124) Halkier, A.; Helgaker, T.; Jørgensen, P.; Klopper, W.; Koch, H.; Olsen, J.; Wilson, A. K., Basis-set convergence in correlated calculations on Ne, N_2, and H_2. *Chem. Phys. Lett.* **1998,** 286, 243-252.

(125) Peterson, K. A.; Dunning, T. H. Intrinsic Errors in Several Ab Initio Methods. The Dissociation Energy of N_2. J. Phys. Chem. 1995, 99, 3898–3901.

(126) Feller, D. Application of Systematic Sequences of Wave Functions to the Water Dimer. *J. Chem. Phys.* **1992,** 96, 6104–611.

(127) Valiev, M.; Bylaska, E. J.; Govind, N.; Kowalski, K.; Straatsma, T. P.; Van Dam, H. J. J.; Wang, D.; Nieplocha, J.; Apra, E.; Windus, T. L.; et al. NWChem: A Comprehensive and Scalable Open-Source Solution for Large Scale Molecular Simulations. *Comput. Phys. Commun.* **2010**, 181, 1477–1489.

(128) Schmidt, J. R.; Polik, W. F. WebMO Enterprise, 17.0.012e; WebMO, LLC.: Holland, MI, 2017 Schuchardt, D.K. Gracio, and B. Palmer.

(129) Vasilyev, V. Online Complete Basis Set Limit Extrapolation Calculator. *Comput. Theor. Chem.* **2017,** 1115, 1–3.

(130) CurveExpert pro 2.6.5, Daniel G. Hyams, Hyam Development Inc.

(131) Zhang B.; HU C.: Introduction to Computational Chemistry; John Wiley & Sons Ltd: West Sussex, 2007; pp 232–264.

APPENDICES

Appendix A: Parameter Values at CBS Extrapolation Limit

Table 7: Parameter values of the CBS extrapolation equations for melatonin, oxidation products, and hydroxyl radical

Molecule	HF_{ECBS1}	HF_{ECBS2}		DFT_{ECBS3}	DFT_{ECBS4}	
	B	B	α	B	B	α
Melatonin	10.8272766	4.7023469	1.4294955	12.5594645	5.9858204	1.4842799
2-OH MLT	12.0984511	5.5901088	1.4660827	14.3152369	7.2303810	1.5181628
4-OH MLT	12.0787585	5.4335080	1.4502972	13.9126410	6.3726962	1.4609637
6-OH MLT	12.1669710	6.5493572	1.5550563	13.9195907	6.0409461	1.4290625
OH Radical	1.3009282	0.5046971	1.3619375	1.6705564	0.3338447	2.8555673
H_2O	1.6338931	0.5934995	1.3219597	2.0812564	0.8942294	1.4231068

Appendix B: Complete Basis Set Extrapolation Curves

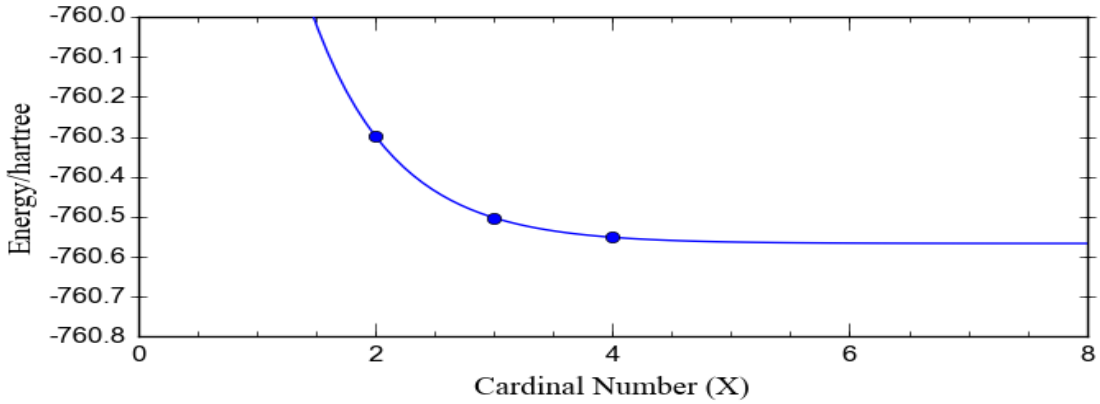

Data name: Data

Dataset source: Unknown

Number of Points: 3

Number of Columns: 2

Statistic	X	Y
Minimum	2	-760.5511874
Maximum	4	-760.2970722
Range	2	0.2541152
Average	3	-760.450119433
Std. Deviation	0.816496580928	0.110060640377

Distributing the calculation over 4 cores...

Final Result [Custom/HF(CBS2) exponential_3_parameters_corrected]:

Equation: -760.5666416+ b* exp (-x* alpha)

b = 4.702306276105102E+00

alpha = 1.429491308529638E+00

Standard Error: 6.464842237753118E-07

Correlation Coefficient: 9.999999999942495E-01

Run time: 0.2490 seconds

Figure 23: Graph of optimized energy of melatonin fit to HF/cc-pVXZ (X=D, T, Q) CBS limit

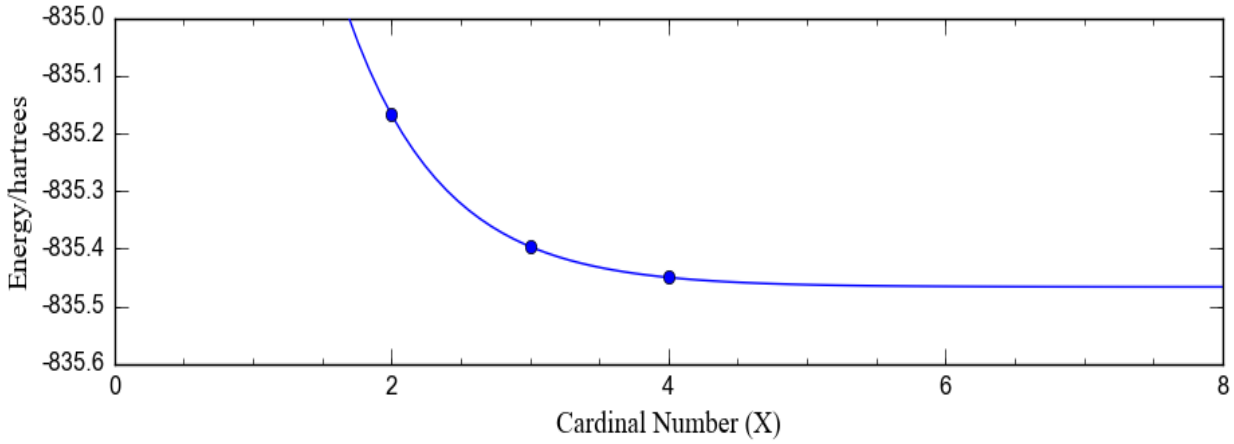

Dataset name: Data
Dataset source: unknown

Number of Points: 3

Number of Columns: 2

Statistic	X	Y
Minimum	2	-835.4566734
Maximum	4	-835.1746939
Range	2	0.2819795
Average	3	-835.345052933
Std. Deviation	0.816496580928	0.122381300357

Final Result [Custom/2-OH(MLT)HF_exponential_3_parameters_corrected]:

Equation: -835.4725435 + b* exp (-x* alpha)

b = 5.590096379772326E+00

alpha = 1.466081589305363E+00

Standard Error: 1.992227897705757E-07

Correlation Coefficient: 9.999999999995584E-01

Run time: 0.0080 seconds

Figure 24: Graph of the optimized energy of 2-OH melatonin fit to HF/cc-pVXZ (X=D, T, Q) CBS limit

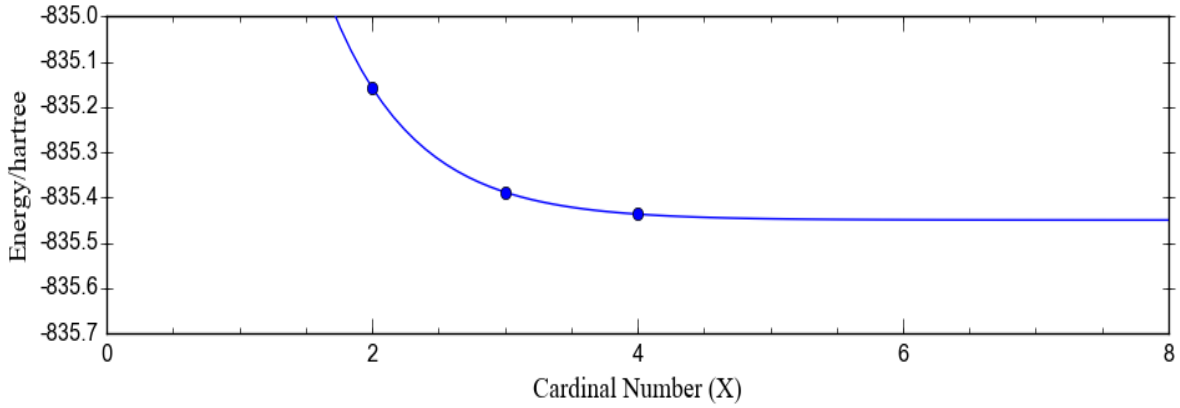

Dataset name: Data
Dataset source: Unknown

Number of Points: 3

Number of Columns: 2

Statistic	X	Y
Minimum	2	-835.4498964
Maximum	4	-835.1675358
Range	2	0.2823606
Average	3	-835.337897567
Std. Deviation	0.816496580928	0.122437878394

Distributing the calculation over 4 cores...

Final Result [Custom/4-OH(MLT)_exponential_3_parameters_corrected]:

Equation: -835.4663273+ b* exp (-x* alpha)

b = 5.433494203371832E+00

alpha = 1.450295864263792E+00

Standard Error: 1.718826202998463E-07

Correlation Coefficient: 9.999999999996715E-01

Run time: 0.0090 second

Figure 25: Graph of the optimized energy of 4-OH melatonin fit to HF/cc-pVXZ (X=D, T, Q) CBS limit

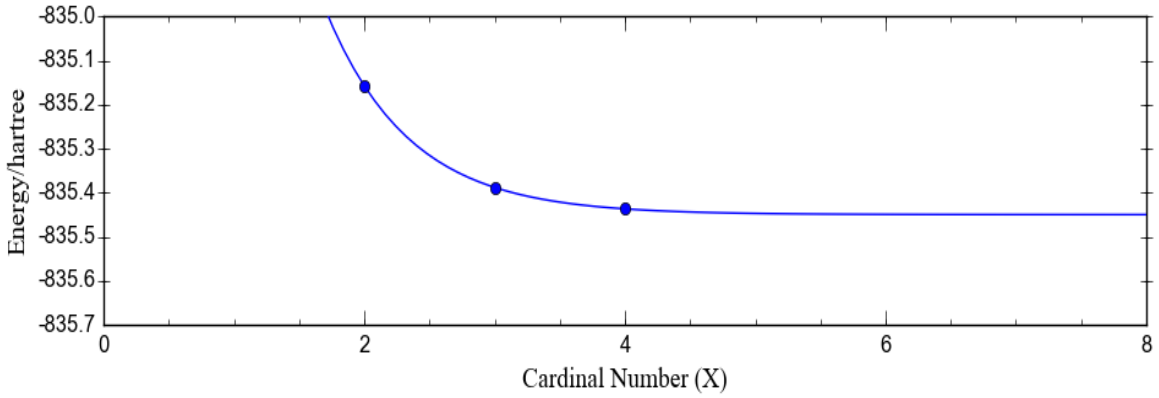

Dataset name: Data

Dataset source: Unknown

Number of Points: 3

Number of Columns: 2

Statistic	X	Y
Minimum	2	-835.43663
Maximum	4	-835.1575534
Range	2	0.2790766
Average	3	-835.3273873
Std. Deviation	0.816496580928	0.121722107839

Final Result [Custom/6-OH(MLT)_exponential_3_parameters_corrected]:

Equation: -835.4496581+ b* exp (-x* alpha)

b = 6.551054499649934E+00

alpha = 1.555134769059839E+00

Standard Error: 3.769264888731280E-06

Correlation Coefficient: 9.999999998401830E-01

Run time: 0.0070 seconds

Figure 26: Graph of the optimized energy of 6-OH melatonin fit to HF/cc-pVXZ (X=D, T, Q) CBS limit

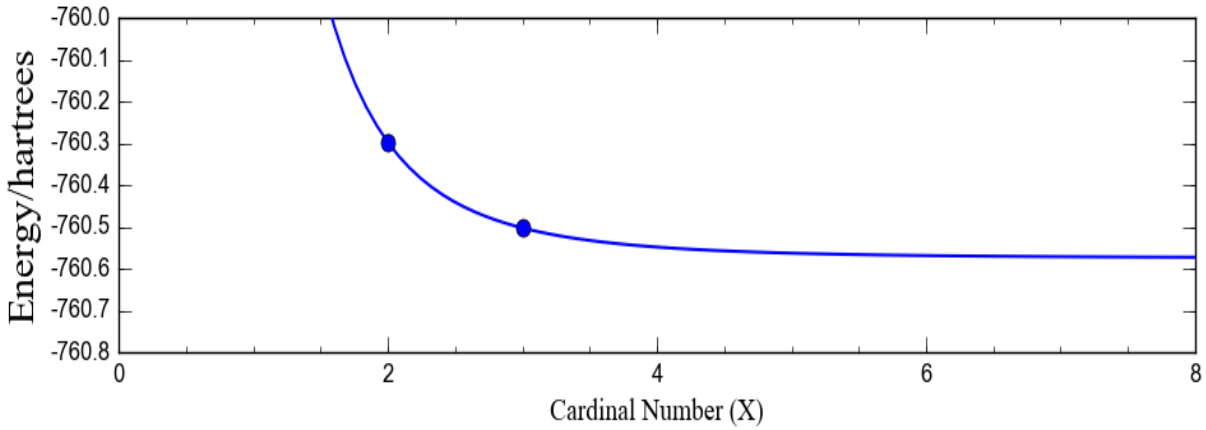

Dataset name: Data

Dataset source: Unknown

Number of Points: 2

Number of Columns: 2

Statistic	X	Y
Minimum	2	-760.5021
Maximum	3	-760.297043
Range	1	0.205057
Average	2.5	-760.3995715
Std. Deviation	0.5	0.1025285

Final Result [Custom/2-parametres_HF(MLT)CBS1)]:

Equation: -760.57426251 + 10.8288873/(x + 1/2)**4

Standard Error: 0.000000000000000E+00

Correlation Coefficient: 0.000000000000000E+00

Figure 27: Graph of the optimized energy of melatonin fit to HF/cc-pVXZ (X=D, T) CBS limit

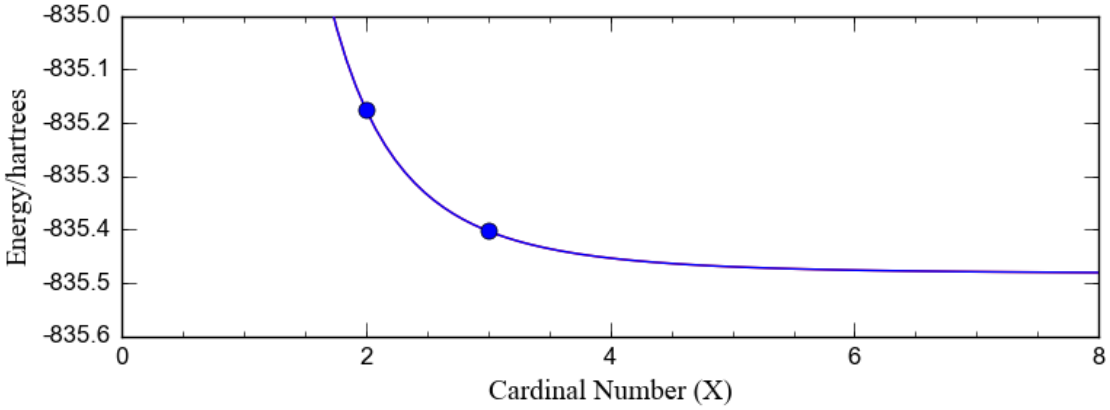

Dataset name: Data

Dataset source: Unknown

Number of Points: 2

Number of Columns: 2

Statistic	X	Y
Minimum	2	-835.402619
Maximum	3	-835.17469
Range	1	0.227929
Average	2.5	-835.2886545
Std. Deviation	0.5	0.1139645

Final Result [Custom/2-parameters(2-OH) CBS1]:

Equation: -835.48283050 + 12.0367383/(x+ 1/2)**4

Standard Error: 0.000000000000000E+00

Correlation Coefficient: 0.000000000000000E+00

Figure 28: Graph of the optimized energy of 2-OH melatonin fit to HF/cc-pVXZ (X=D, T) CBS limit

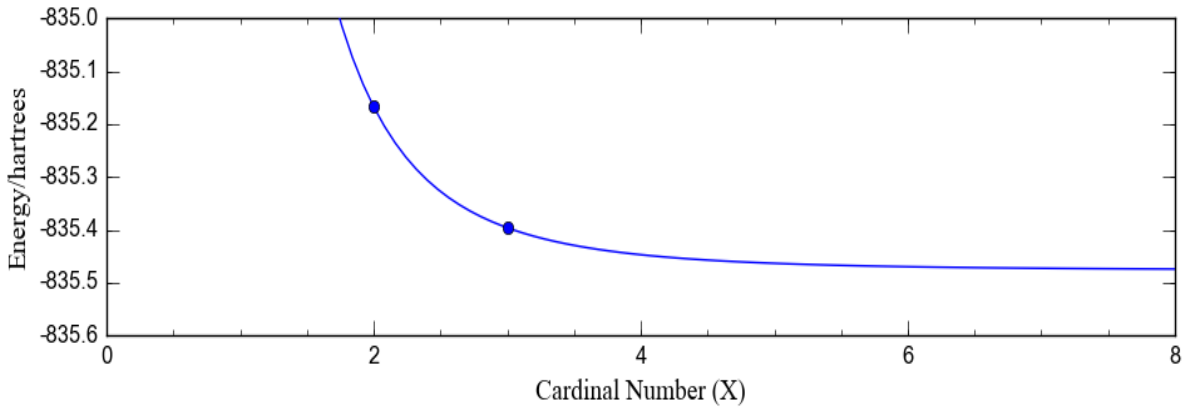

Dataset name: Data

Dataset source: Unknown

Number of Points: 2

Number of Columns: 2

Statistic	X	Y
Minimum	2	-835.3962605
Maximum	3	-835.1675358
Range	1	0.2287247
Average	2.5	-835.28189815
Std. Deviation	0.5	0.11436235

Final Result [Custom/4-OH(MLT)HFCBS1(2-prameters)]:

Equation: -835.476752 +12.0787585/(x +1/2)**4

Standard Error: 0.000000000000000E+00

Correlation Coefficient: 0.000000000000000E+00

Figure 29: Graph of the optimized energy of 4-OH melatonin fit to HF/cc-pVXZ (X=D, T) CBS limit

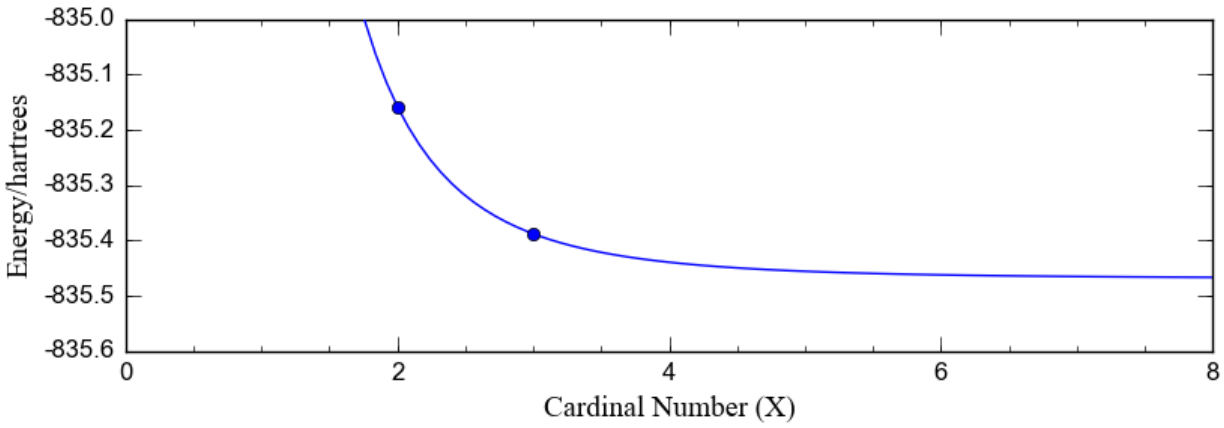

Dataset name: Data

Dataset source: Unknown

Number of Points: 2

Number of Columns: 2

Statistic	X	Y
Minimum	2	-835.3879785
Maximum	3	-835.1575834
Range	1	0.2303951
Average	2.5	-835.27278095
Std. Deviation	0.5	0.11519755

Final Result [Custom/6-OH(HF)(MLT)CBS1)2-Parameter]:

Equation: -835.4690579+ 12.1669710/(x+1/2)**4

Standard Error: 0.000000000000000E+00

Correlation Coefficient: 0.000000000000000E+00

Figure 30: Graph of the optimized energy of 6-OH melatonin fit to HF/cc-pVXZ (X=D, T) complete basis set limit

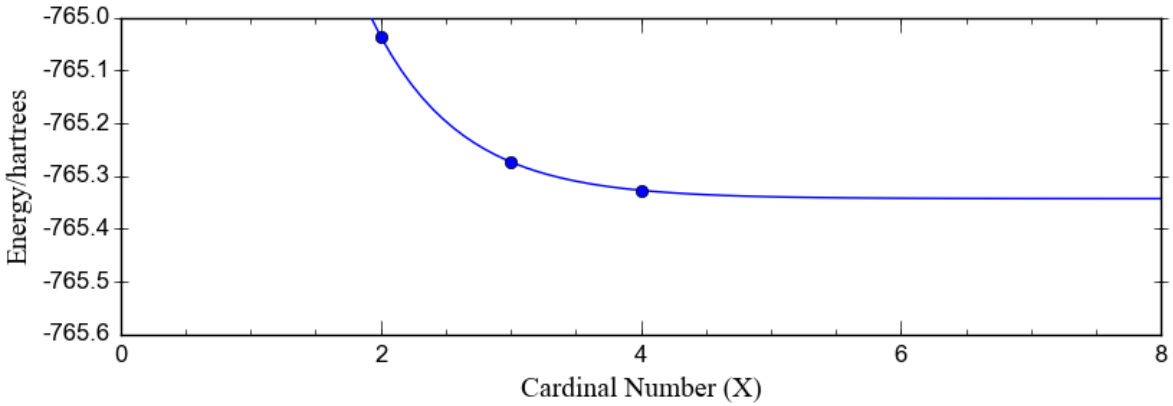

Dataset name: Data

Dataset source: Unknown

Number of Points: 3

Number of Columns: 2

Statistic	X	Y
Minimum	2	-765.3270563
Maximum	4	-765.0353218
Range	2	0.2917345
Average	3	-765.211842433
Std. Deviation	0.816496580928	0.126744215784

Final Result [Custom/MLTDFT_(CBS4) exponential_3_parameters_corrected]:

Equation: -765.3428568 + b* exp (-x* alpha)

b = 5.985803868390095E+00

alpha = 1.484278523326851E+00

Standard Error: 1.694222451222464E-07

Correlation Coefficient: 9.999999999997021E-01

Run time: 0.1760 seconds

Figure 31: Graph of the optimized energy of melatonin fit to DFT/B3LYP/cc-pVXZ (X=D,T,Z) CBS limit

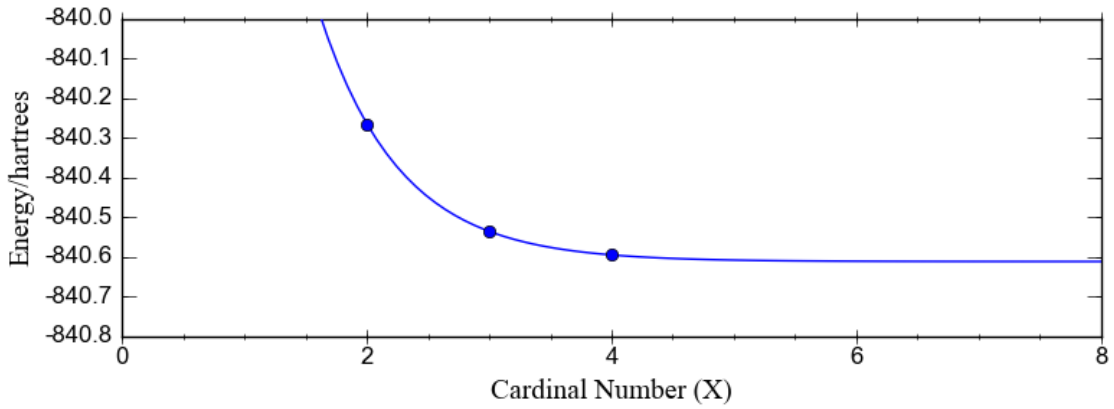

Dataset name: Data

Dataset source: Unknown

Number of Points: 3

Number of Columns: 2

Statistic	X	Y
Minimum	2	-840.5952905
Maximum	4	-840.2648193
Range	2	0.3304712
Average	3	-840.465334667
Std. Deviation	0.816496580928	0.143844335575

Final Result [Custom/2-OHMLTDFT_(CBS4)exponential_3_parameters_corrected]:

Equation: -840.6119569 + b* exp (-x* alpha)

b = 7.230386241823301E+00

alpha = 1.518163246310894E+00

Standard Error: 6.185050047778878E-10

Correlation Coefficient: 1.000000000000000E+00

Run time: 0.0180 seconds

Figure 32: Graph of the optimized energy of 2-OH melatonin fit to DFT/B3LYP/cc-pVXZ (X=D, T, Z) CBS limit

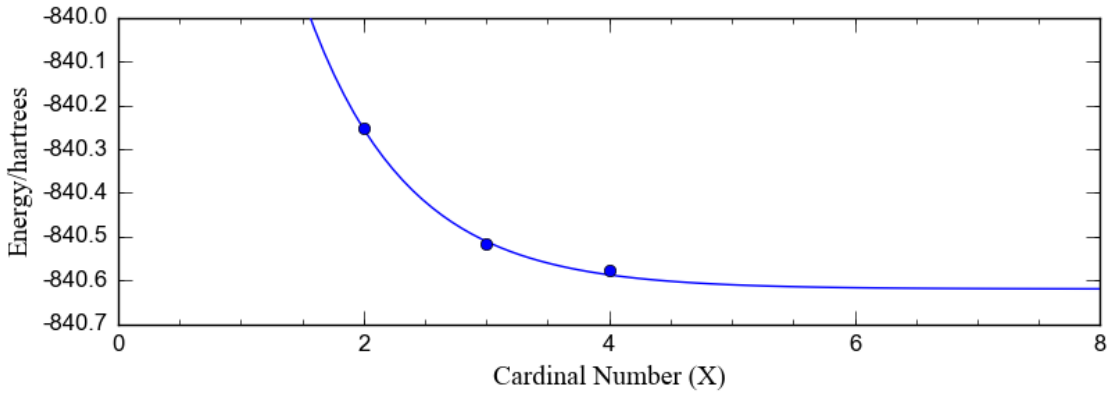

Dataset name: Data

Dataset source: Unknown

Number of Points: 3

Number of Columns: 2

Statistic	X	Y
Minimum	2	-840.5777565
Maximum	4	-840.2531812
Range	2	0.3245753
Average	3	-840.449190067
Std. Deviation	0.816496580928	0.140827655198

Final Result [Custom/4-OH(MLT)DFTCBS4_exponential_3_parameters_corrected]:

Equation: -840.61958393+ b* exp (-x* alpha)

b = 4.140030692998351E+00

alpha = 1.213514606112460E+00

Standard Error: 1.113998662535561E-02

Correlation Coefficient: 9.989565567550535E-01

Run time: 0.0470 seconds

Figure 33: Graph of the optimized energy of 4-OH melatonin fit to DFT/B3LYP/cc-pVXZ (X=D, T, Z) complete basis set limit

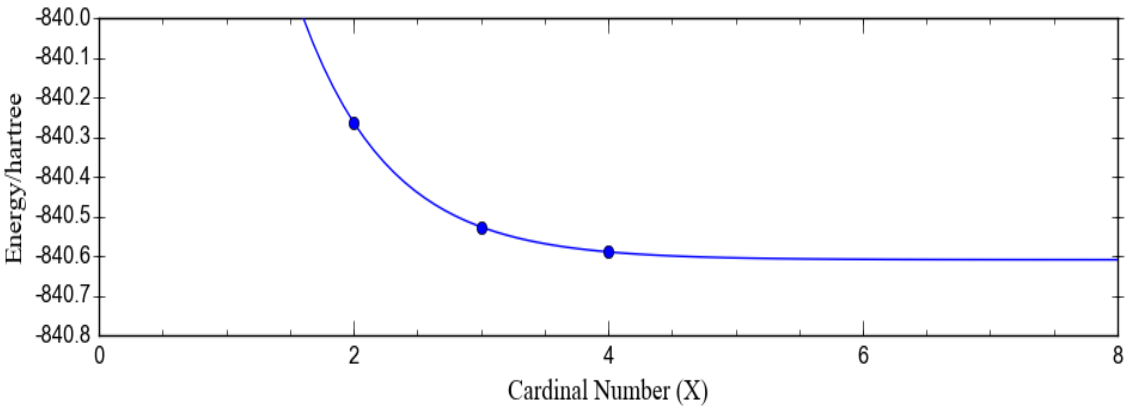

Dataset name: Data

Dataset source: Unknown

Number of Points: 3

Number of Columns: 2

Statistic	X	Y
Minimum	2	-840.5892312
Maximum	4	-840.2625114
Range	2	0.3267198
Average	3	-840.459278967
Std. Deviation	0.816496580928	0.14150305887

Final Result [Custom/6-OHMLTDFT_(CBS4) exponential_3_parameters_corrected]:

Equation: -840.6091182 + b* exp (-x* alpha)

b = 6.040946061014567E+00

alpha = 1.429062457800492E+00

Standard Error: 3.794734531838099E-09

Correlation Coefficient: 9.999999999999999E-01

Run time: 0.0160 seconds

Figure 34: Graph of the optimized energy of 6-OH melatonin fit to DFT/B3LYP/cc-pVXZ (X=D, T, Z) CBS limit

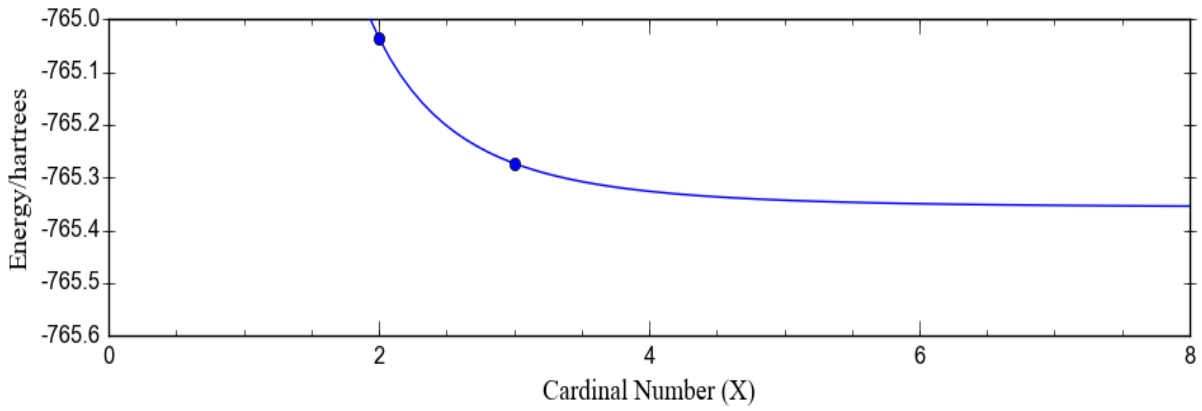

Dataset name: Data

Dataset source: Unknown

Number of Points: 2

Number of Columns: 2

Statistic	X	Y
Minimum	2	-765.2731492
Maximum	3	-765.0353218
Range	1	0.2378274
Average	2.5	-765.1542355
Std. Deviation	0.5	0.1189137

Final Result [Custom/DFT(MLT)CBS3)2-parametres_]:

Equation: -765.3568441 + 12.5594645/(x + 1/2)**4

Standard Error: 0.000000000000000E+00

Correlation Coefficient: 0.000000000000000E+00

Figure 35: Graph of the optimized energy of melatonin fit to DFT/B3LYP/cc-pVXZ (X=D,T) CBS limit

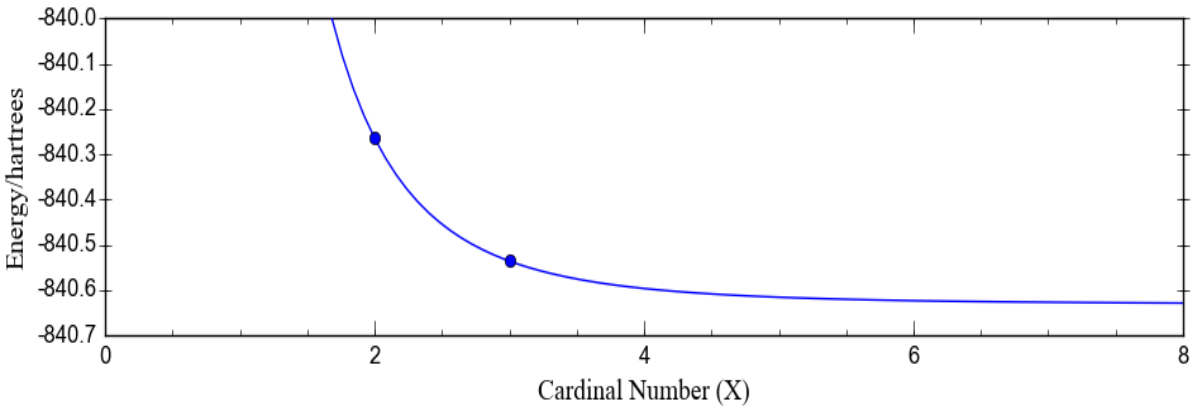

Dataset name: Data

Dataset source: Unknown

Number of Points: 2

Number of Columns: 2

Statistic	X	Y
Minimum	2	-840.5358942
Maximum	3	-840.2648193
Range	1	0.2710749
Average	2.5	-840.40035675
Std. Deviation	0.5	0.13553745

Distributing the calculation over 4 cores...

Final Result [Custom/DFT(2-OHMLT) CBS3)2-parametres_]:

Equation: -840.6312894 + 14.3152369/(x + 1/2)**4

Standard Error: 0.000000000000000E+00

Correlation Coefficient: 0.000000000000000E+00

Figure 36: Graph of the optimized energy of 2-OH melatonin fit to DFT/B3LYP/cc-pVXZ (X=D, T) complete basis set limit

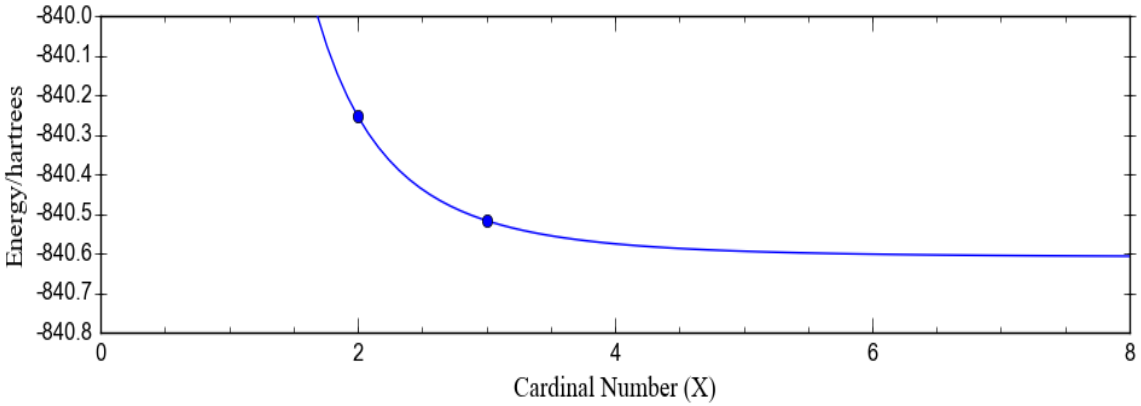

Dataset name: Data

Dataset source: Unknown

Number of Points: 2

Number of Columns: 2

Statistic	X	Y
Minimum	2	-840.5166325
Maximum	3	-840.2531812
Range	1	0.2634513
Average	2.5	-840.38490685
Std. Deviation	0.5	0.13172565

Distributing the calculation over 4 cores...

Final Result [Custom/DFT(4-OH-MLT)CBS3)2-parametres_]:

Equation: -840.6093448+ 13.9126410/(x + 1/2)**4

Standard Error: 0.000000000000000E+00

Correlation Coefficient: 0.000000000000000E+00

Figure 37: Graph of the optimized energy of 4-OH melatonin fit to DFT/B3LYP/cc-pVXZ (X=D, T) CBS limit

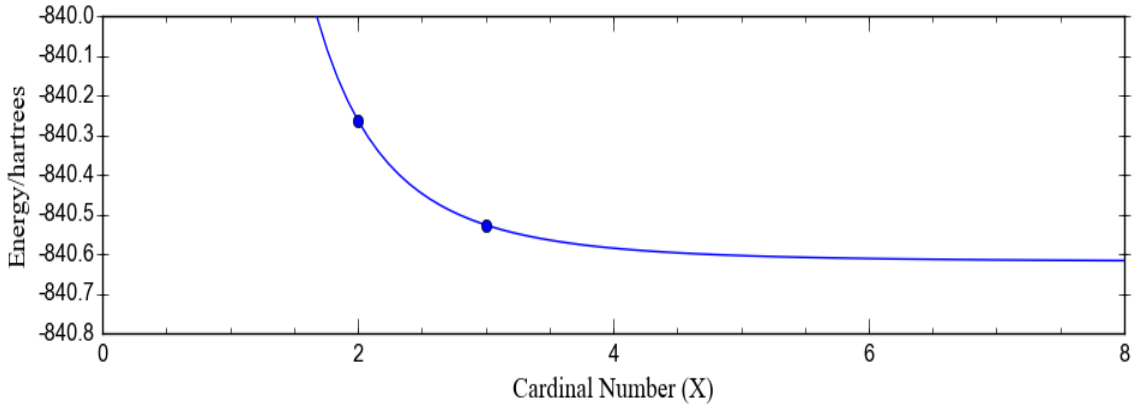

Dataset name: Data

Dataset source: Unknown

Number of Points: 2

Number of Columns: 2

Statistic	X	Y
Minimum	2	-840.5260943
Maximum	3	-840.2625114
Range	1	0.2635829
Average	2.5	-840.39430285
Std. Deviation	0.5	0.13179145

Final Result [Custom/DFT(6-OH-MLT) CBS3)2-parametres_]:

Equation: -840.6188529+ 13.9195907/(x + 1/2)**4

Standard Error: 0.000000000000000E+00

Correlation Coefficient: 0.000000000000000E+00

Figure 38: Graph of the optimized energy of 6-OH melatonin fit to DFT/B3LYP/cc-pVXZ (X=D, T) CBS limit

VITA

OLADUN SOLOMON OLADIRAN

Education:	M.S. Chemistry, East Tennessee State University, Johnson City, TN, 2020
	B.S. Petroleum and Petrochemical Science, Tai Solarin University of Education, Ogun State, Nigeria, 2013
Professional Experience:	Graduate Teaching Assistant, East Tennessee State University, Department of Chemistry, 2017-2019
	Chemistry/Mathematics Teacher, STC Model Academy, Surulere, Lagos, Nigeria, 2015-2017
Poster Presentation	Oladiran, O.S.; Kirkby, S.J. Computational Studies of the Spin Trapping Behavior of Melatonin and its Derivatives. Presented at the Appalachian Student Research Forum, Johnson City, TN, April 12, 2019
	Oladiran, O.S.; Kirkby, S.J. Computational Studies of the Spin Trapping Behavior of Melatonin and its Derivatives. Presented at the 75th Southwest, and 71st Southeast Joint Regional Meeting of the American Chemical Society, Savannah GA, October 20-23, 2019